Locomotion and muscle fiber distribution in mammals

哺乳類のロコモーションと筋線維分布

The United Graduate School of Veterinary Science

Yamaguchi University

Hiroshi ICHIKAWA

March 2019

Preface

The aim of this research is to examine the relationship between locomotion characteristics of mammals and their anatomical structure of musculoskeletal system, and biochemical and physiological distribution of muscle fibers.

Locomotion is the active movement from one place to another. Creatures which have ability of locomotion are called “Animal”. To achieve locomotion, animals have motor system and sensory systems which sense changes in the external environment. Animals move to search for bait or prey, to escape from predators, to find a breeding partner to leave offspring, or to find the environment more suitable for maintaining their life. Locomotion is a life activity using the basic whole body of animals. The trouble with function for locomotion means that the animal surely approaches death in the natural world.

It is thought that mammalian ancestry had emerged on the earth about 250 million years ago after passing through the ancestors of fish, amphibians, reptiles (synapsid). Mammals and birds are vertebrate animals highly adapted to the terrestrial environment. Mammals have a “homeothermism” mechanism to keep the body temperature within a certain range. By maintaining a high level of chemical reaction in the body with constant temperature, the energy generated as a result and locomotion is

performed using the energy. Mammals acquire information on various external environments through developed sensory organs, and it makes them possible to perform dynamic and beautiful locomotion using elaborate motile organs. Mammals have extremely advanced adaptive abilities and expanded their habitats into various environments on the planet. Today, about 5500 species of mammals live in different environments on this planet. Mammals live everywhere on the planet; on the land, in the water, in the various climate zones, on the trees, and also underground. This habitat diversity is a characteristic of mammals. Mammals perform species-specific and variety types of locomotion in order to maintain life and preserve offspring in their habitat. As a characteristic of mammalian locomotion, the remarkable difference from fish, amphibian or reptiles is that the movement is three dimensional. Three-dimensional movement, which is combination of up-and-down and forward-and-backward movements, is produced from the shape of the mammalian body. Elbows and knees of amphibians or reptiles are located outside of the trunk. Mammals, on the other hand, have long legs beneath the trunk, and elbows and knees are right under the trunk. Animals moving on land utilize the force received on the sole of the foot, which is called the ground reaction force, to support the body and to perform locomotion. In the body types of amphibians or reptiles, the ground reaction force works on the knees and

elbows but not directly to the trunk. On the other hand, in mammals, the force from the ground works directly on the trunk via elbows and knees, so it works as the force to lift the trunk.

Animals move their bodies to perform locomotion. Mammalian motion is created by the tension generated by skeletal muscle in the same way of other vertebrates. Skeletal muscle consists of elongated striated muscle fibers. A large number of myofibrils are arranged in the muscle fibers parallel to its long axis. Myofibril is a series of sarcomere composed of cytoskeletons, which are actin filaments and myosin filaments. Biding of the two filaments to increase the number of crossing (connecting) sites and rotation of the myosin head on the myosin side of the binding part generate sarcomere shortens (slides). The Z disk, which is the border of the sarcomere, is bound to the cell membrane. So, the sliding of the two filaments generates the tension of the muscle fibers. Therefore, the greater the number of myofibrils, the greater the tension produced by the muscle fibers, and the longer the myofibrils, the faster the speed of contraction. Although sliding of actin and myosin and their binding generate tension, the sliding of actin and myosin filaments is not uniform; there are various types of binding, e.g. fast or slow and persistently maintaining or in a short time, and muscle fibers can be classified based on these characteristics. For a long time, mammalian

muscle fibers have been classified by their metabolic (muscle energy converting) enzymes such as ATPase and SDH. In recent years, classifications by types of myosin heavy chain (MHC-isoform), which is decisive for the contraction speed, using MHC-isoform antibodies and by molecular weight of myosin protein fractionated by electrophoresis are used. Muscle fibers are classified as Type I, IIa, IIx, Iib by MHC-isoforms. Furthermore, it can be classified into its intermediate (hybrid) types, type I / IIa (Type C), IIa / IIx, and IIx / IIb.

According to the order of Type I, IIa, IIx and IIb, the contraction speed increases, and the contraction time becomes shorter. The contraction energy of Type I and IIa is aerobic, and that of IIx and IIb is due to glycolytic energy. Aerobic myofibers, I and IIa, have high fatigue resistance, and glycolytic muscle fibers, IIx and IIb, have low fatigue resistance. That indicates, in terms of the tension with respect to the continuous stimulus, the change in the tension of the aerobic muscle fiber is small, and a remarkable decrease in the maximum tension occurs in the muscle fiber with the glycolytic system. Many of studies have reported that the distribution of muscle fibers is closely related to locomotion of animals and the diversity of locomotion in mammals corresponds to the diversity of distribution of muscle fibers.

The purpose of our research is to clarify the characteristics of mammal

locomotion and to examine the relationship with muscle fiber distribution.

Outline of research method [Details are described in each paper]

1) Kinematics and kinetic analysis of locomotion

Photograph shootings were done in the zoo, its related facilities, and the laboratory. Although all mammals possible for the shooting were the subjects of our research, we will present the analysis results of cheetah in this thesis (Ichikawa et al. 2018 Mam. Study)

Kinematic analysis

Kinematic is to analyze visible changes in the shape of the animals, that is, to analyze the movements and quantify them as numerical values. As mammalian locomotion is fast generally, a high-speed camera should be used for shooting. In our research, Casio F1 was used at the frame rate of 300 to 1000 f / s and the following items were examined.

Cycle period analysis / Duty factor

The cycle period of locomotion on the ground can be calculated with examination of contact phase (stance phase), and release phase (swing phase). The ratio of the time of the stance phase to the time required for one cycle is called Duty Factor [dimensionless number]. The animal maintains its posture and performs locomotion using Ground Reaction Force (GFR). As GRF is proportional to the duty factor, an increase in duty factor causes an increase in GRF.

Analysis of joint angle

Analysis of joint angle becomes possible in the case where the positional relationship between the camera and each part of the subject is constant. Using the analysis software, the image and the stick figure are created. Creating the stick figure reveals changes in joint angles.

Kinetic analysis

Kinetic analysis is a method to measure and calculate the exchange of invisible force between the foot and the ground.

Method using the force plate

The force plate is an instrument that measures the ground reaction forces generated by the animal standing on or moving across them. The reaction that the foot acts on the floor is decomposed into forces of the three axes, vertical, front-and-rear and left-and-right directions, to be displayed.

Measurement of acceleration

During locomotion, the animal moves by highly coordinated movement of its body parts. That is, forces acting on each part are converged to one direction and its resultant force creates stable locomotion. The force acting can be measured by placing an acceleration sensor in each part and the motion with an angular velocity sensor, accordingly.

2) Biochemical and physiological study of skeletal muscle,

For the experiment, mammalian individuals immediately after sacrifice (large amount of pentobarbital Na solution) and within 3 days in refrigerated condition were used. 25 to 60 samples were taken from the central portion of the muscle for each individual using a scalpel and rapid freezing with liquid nitrogen after the collection

was performed. After making serial sections with a microtome and colored by reaction with myosin heavy chain antibody with conventional method, microscopic photography was taken. By using the photograph, about 500 muscle fibers from one muscle were classified into the designated types (Type I, IIa, IIx, IIb). We also measured the cross sectional area of the muscle fibers and calculated proportion and average cross-sectional area for each type. In this thesis, I will introduce analysis results of data of moles (Ichikawa et al. 2018 Anat. Rec)

3) Measurement of muscle tension

For muscle tension measurement, moles (Japanese large mole), rats [Wister type], and Sunkus (Asian house shrew) were used. Animals were injected with 45 to 60 mg / kg of Nembutal intraperitoneally. A tracheal tube was inserted for air away maintenance. The depth of anesthesia was judged by the presence of eyelid reflex and flexion reflex of limbs, hand, and additional injection was performed to maintain the depth of anesthesia. Muscle tension was measured by attaching a bipolar stimulation electrode to the isolated sciatic nerve. The stimulus duration in single stimulation was 0.3 ms and continuous stimulation for one minute was performed with 0.1 Hz to 100 Hz frequency.

The stimulation intensities given were 1.0, 1.2, 1.3, 1.5, 2.0, 3.0, 5.0, 10.0 and 20.0 fold of the electro intensity which leads minimal twitch. All maximum tensions appeared within 2.0 fold.

Analysis

For single stimulation, averaging for eight times were performed, and the maximum tension (Tmax), the time to maximum tension (T1), and the relaxation time were measured.

Regarding the effects of continuous stimulation, changes in tension were analysed. (Ichikawa et al. In preparation)

Research organization

This research is underway with the cooperation of Professor Naomi Wada, Assistant professor Yasuo Higurashi, Mr. Masao Matsuo and research students at Laboratory of System Physiology, Joint Faculty of Veterinary Medicine, Yamaguchi University, Japan. In the laboratory, all members are studying the relationship between mammalian locomotion and muscle fiber distribution using analytical methods of kinetics, kinematics, muscle physiology, neurophysiology. In addition, we had supports

from external collaborators, including Dr. Shinichiro Kawata at National Science Museum, Mr. Satoshi Une at Osaka VR Center, Ms. Megumi Haitani, Veterinarian at Akiyoshidai Safari Park, Ashitani Chichibu, Himeji Central Park, Shimonoseki Aquarium Kaikyokan, Shunan City Tokuyama Zoo, Hiroshima City Asa Zoo, Fukuoka City Zoological and Botanical Garden, Miyazaki City Phoenix Zoo and Tama Zoological Park.

Kinematic Studies

Gait characteristics of cheetahs (*Acinonyx jubatus*) and greyhounds (*Canis lupus familiaris*) running on curves

Introduction

Success in hunting prey and escaping from predators, which greatly affect fitness, depends on many factors. One factor is maximum speed. The faster animals run, the greater the possibility of successful hunting and escape. Another factor is the ability to make a turn at high speeds. Prey species of cursorial carnivores often attempt to escape by abruptly changing directions just before they are caught up with by the predator (Alexander 2003). An experimental study using a tablet-based game that simulated predator-prey chases found that both speed and turning ability affected escape success (Clemente and Wilson 2016). Most studies on legged locomotion have focused on walking and running in a straight line at a steady speed. As turning ability is important for survival success, knowledge of the biomechanics of turning at high speeds helps us to further our understanding of form-function relationships in animals. To this end, we investigated gait characteristics of the cheetah (*Acinonyx jubatus*) and greyhound (*Canis lupus familiaris*) while running in a straight line and on curves.

Interspecific comparisons present an opportunity to clarify whether strategies to deal with curve running differs between the cheetah and greyhound, both of which are characterized by superior sprinting ability. The cheetah is well known as the fastest land animal in the world and has morphological adaptations for high-speed locomotion (Russell and Bryant 2001; Hudson et al. 2011a, 2011b; Goto et al. 2013; West et al. 2013). In experimental conditions where food reward was used to encourage a cheetah to run in a straight line, the top speed was 29 m s^{-1} (Sharp 1997). During hunting in the wild, the top speed of 25.9 m s^{-1} was recorded (Wilson et al. 2013a). However, cheetah hunts are composed not only of maximum speed chases, but also of decelerating and turning with appropriate timing (Wilson et al. 2013b). The greyhound is one of the fastest dog breeds, and its hindlimbs are adapted for sprinting (Williams et al. 2008a, 2008b). The published running speed during a race was 16.45 m s^{-1} (Zebas et al. 1991). Straight running by the cheetah and greyhound has been examined in detail by Hudson et al. (2012) using high-speed video and force plate analysis.

At high speeds, the cheetah and greyhound use a form of gallop referred to as the rotatory gallop (Hildebrand 1959, 1977; Biancardi and Minetti 2012). In the rotatory gallop, landing and take-off are from ipsilateral limbs of each left-right pair. Specifically, the limbs make contact with the ground in the order of left fore, right fore, right hind,

left hind (clockwise) or right fore, left fore, left hind, right hind (counterclockwise). The limb of a left-right pair that is the first to contact the ground is referred to as the non-lead limb or trailing limb. The contralateral limb is referred to as the lead limb. When animals gallop, they allocate biomechanical tasks unevenly among the limbs. In the rotatory gallop in the cheetah and greyhound at the speed of 18 m s^{-1}, the hindlimbs support a greater proportion of body weight than the forelimbs, with the non-lead and lead limbs contributing unequally to this task (Hudson et al. 2012).

The biomechanical demands of curve running differ from those of straight running. Animals running on curves must produce centripetal forces to change velocity heading in the new direction (Daley 2016). Several insights into the mechanics of curve running have been derived from experiments on humans. The maximum running speed on curves of differing radii (1–37.72 m) is slower compared with straight running (Chang and Kram 2007; Churchill et al. 2016; Taboga et al. 2016). In addition, the limb on the inside of the curve has a longer contact time and generates lower peak resultant ground reaction forces (GRFs) compared with the outside limb and the limbs during straight running (Chang and Kram 2007; Churchill et al. 2016). The factor that limits maximum curve-running speed is still controversial (Usherwood and Wilson 2006; Chang and Kram 2007; Churchill et al. 2016). However, lower peak resultant forces

exerted by the inside limb indicate that the additional requirement to produce centripetal forces is not the sole limiting factor. Two studies have compared curve and straight running in the greyhound. Usherwood and Wilson (2005) reported that greyhounds did not slow down on curves compared with straight running. In contrast, Hayati et al. (2017) found that stride length was shorter during curve running with similar stride frequency between the two running conditions. As speed is the product of stride length and stride frequency, their results indicated slower speeds on curves. Further studies are needed to account for this discrepancy.

In this study, we determined footfall patterns during straight and curve running in the cheetah and the greyhound. We then determined the duty factor, or relative limb contact time, for each limb. The duty factor is an important variable in studies of legged locomotion. This variable serves as a measure of the relative time allotted for reaccelerating and redirecting the center of mass of the body (Biknevicius and Reilly 2006). It was also used to predict the peak vertical GRF during equine locomotion (Witte et al. 2004). Finally, we evaluated interlimb coordination using the framework proposed by Abourachid (2003), which is explained in the following section, to discuss how much capacity animals have to change interlimb coordination to meet the changing demands of running.

Materials and methods

Four adult male cheetahs and four adult male greyhounds were the subjects in this study. These animals were housed at a zoo (Shanghai Wild Animal Park, China). The cheetahs were raised from infancy at the zoo. All experimental protocols were approved by the Institutional Animal Care and Use Committee at Yamaguchi University.

Experiments were conducted at the zoo. The cheetahs and greyhounds were encouraged to run around a 400-m track using a lure that travels ahead of them on the inside rail (Fig. 1A, B). The track was oval-shaped and composed of two 80-m straights that never cross connected by two bends with a radius of 38 m. The animals started from one corner between the bend and the straight, and ran the straight first and then the bend. The animals ran the track in a counterclockwise direction. The speed of the lure was controllable and set to 15–18 m s^{-1}. According to the study by Hudson et al. (2012), the cheetah and greyhound use a gallop at these high speeds. Video recordings were made using eight high-speed cameras: two MEMRECAM HX-7 cameras (nac Image Technology, Tokyo, Japan) and six EX-F1 cameras (CASIO, Tokyo, Japan). The cameras filmed the animals from a lateral or diagonal view with a frame-rate of 1,000 or 1,200 frames s^{-1}.

We analyzed gait characteristics in 47 straight-running strides and 37 curve-running strides of the cheetahs, and in 19 straight-running strides and 22 curve-running strides of the greyhounds. The stride period was defined as the time elapsed between two consecutive touchdowns of the non-lead forelimb. The time of touchdown and liftoff of each limb during a stride were determined. The duty factor was calculated as the stance period relative to the stride period. In addition, the fore lag and hind lag were measured (Fig. 1C). These temporal parameters were proposed by Abourachid to quantify interlimb coordination and identify quadrupedal gaits (Abourachid 2003; Abourachid et al. 2007). The fore lag was defined as the time between the touchdowns of the non-lead and lead forelimbs, and the hind lag was defined as the time between the touchdowns of the non-lead and lead hindlimbs.

All statistical tests were performed using OriginPro 2017 (LightStone, Tokyo, Japan). The Student's unpaired *t* test was used to evaluate differences between straight and curve running for each limb within a species. The level of significance was set at $\alpha = 0.05$. Data are presented as the mean ± SD.

Results

In all strides analyzed, the cheetahs and the greyhounds used the rotatory gallop (Figs. 2A and 3), and the order of footfalls was variable during straight running and was constant during curve running. During straight running in the cheetahs, the footfall order of the rotatory gallop was clockwise in 21 strides and counterclockwise in 26 strides. During curve running in a counterclockwise direction, the footfall order was always counterclockwise (Fig. 2B). In this order, the non-lead forelimb was the right forelimb, and the non-lead hindlimb was the left hindlimb. During the curve-running task used in this study, the right limbs were on the outside and the left limbs were on the inside of the curve. Similarly, during curve running in the greyhounds, the footfall order of the rotatory gallop was invariably counterclockwise.

The effects of curves on the duty factor of an individual limb differed between the two species (Table 1). In the cheetahs, the duty factor of the non-lead and lead forelimbs, and the lead hindlimb did not significantly change during curve running compared with straight running. However, the duty factor of the non-lead hindlimb was significantly greater during curve running. In the greyhounds, the duty factor of the non-lead hindlimb did not significantly differ between the two running conditions. The duty factor of both forelimbs was significantly greater during curve running. The duty

factor of the lead hindlimb was greater during curve running, although the difference was not significant ($P = 0.055$).

The effects of curves on interlimb coordination also varied between the cheetah and greyhound (Table 2). In the cheetahs, the fore lag did not significantly differ between straight and curve running. However, the hind lag was significantly longer during curve running. In the greyhounds, the fore and hind lags did not significantly differ between the two running conditions.

Discussion

We report three major findings. Firstly, the footfall order was fixed during curve running, although it was variable while running straight. Both the cheetah and greyhound used a rotatory gallop with a counterclockwise footfall pattern in all curve-running strides analyzed, while running the track counterclockwise. Secondly, the duty factor increased on curves compared with straight running only for the non-lead hindlimb in the cheetah, but for three out of the four limbs in the greyhound (Table 1). As the animals ran the track in a counterclockwise direction, the non-lead hindlimb was the left limb on the inside of the curve. Lastly, the coordination between the non-lead and lead hindlimbs changed with different running conditions in the cheetah, whereas

interlimb coordination did not change significantly in the greyhound (Table 2). Furthermore, it is important to note two limitations of this study. Firstly, our study did not measure the running speed of the animals for each stride. This limitation does not allow us to discuss interspecific differences in curve-running performance as defined by maximum curve-running speed relative to maximum straight-running speed. Secondly, we could not identify the animals recorded in video clips individually because they were similar in appearance. As a result, we pooled data from different individuals of the same species and do not discuss the inter-individual variation in the duty factor and interlimb coordination.

This study demonstrates that both the cheetah and greyhound fix the rotatory gallop footfall order during curve running using a counterclockwise sequence of footfalls, in the order of right fore, left fore, left hind, right hind, on curves when running the track in a counterclockwise direction. This finding is in agreement with Hildebrand's (1977) findings, which showed that the inside forelimb was used as the lead limb when turning. A preference for one footfall order during curve running is also observed in horses, which use a transverse gallop rather than the rotatory gallop. Horses show a preference for the inside limb as the lead limb despite the direction of the curve (Hildebrand 1980; Williams and Norris 2007; Barrey 2013). Thus, the use of the inside

forelimb as the lead forelimb is common in both rotatory and transverse galloping. It is believed that horses maintain balance more easily on the inside lead than the outside lead (Hildebrand 1980; Barrey 2013). Similar factors may affect the choice of footfall order in the cheetah and greyhound. It is of interest to investigate whether the cheetah and greyhound use the clockwise footfall sequence on curves when running a track in a clockwise direction. However, to the best of our knowledge, no one has provided a mechanical explanation for why the inside lead of the forelimb improves balance on curves. In both forms of gallop, the lead forelimb is the last limb to leave the ground before the crossed flight phase when animals cannot generate GRF (Fig. 2A; Bertram and Gutmann 2009; Biancardi and Minetti 2012). Therefore, the inside lead of the forelimb may be related to fine adjustments of speed and direction during the crossed flight phase.

Two studies reported the duty factor during high-speed running in the cheetah and/or greyhound. Hudson et al. (2012) presented a graph showing the duty factor for the non-lead forelimb during straight running in the cheetah and the greyhound. Within the range of speeds covered in this study (15–18 m s^{-1}), the results of Hudson et al. (2012) and our results show similar values. This concordance supports the validity of our measurements. On the other hand, the duty factor in the greyhound reported by

Usherwood and Wilson (2005) is generally smaller than that in our study despite the similar speeds. Some differences in methodology exist across studies. The camera frame rate was 250 frames s^{-1} in the study by Usherwood and Wilson (2005). We used high-speed cameras that enabled a finer time resolution, at 1,000 or 1,200 frames s^{-1}. The radius of the track used by Usherwood and Wilson (2005) was 22.4 m, but was 38 m in this study.

The percentage-point differences (up to 2.5 percentage points) in the duty factor and hind lag between running conditions may seem trivial (Tables 1 and 2). However, only a short time is available during high-speed locomotion to change speed and direction. For greyhounds running straight at speeds of 15.19–16.33 m s^{-1}, the stride period is 283.7–292.4 ms, and the contact time of individual limbs in a stride is 40.2–50.8 ms (Usherwood and Wilson 2005). Stuart et al. (1973) showed that a large change in the galloping speed (from 4.63 to 5.82 m s^{-1}) of a cat on a treadmill was related to a relatively small change in absolute and relative limb contact time. Therefore, the observed differences between running conditions in this study merit consideration.

The interspecific differences in the effects of curves on the duty factor and interlimb coordination suggest that the cheetah and greyhound use different strategies to deal with curve running. Animals running on curves continuously change velocity

heading in the intended direction of travel. The results from previous experiments on humans suggest functional differences in the role of the limbs during curve running. Churchill et al. (2016) demonstrated that the inside limb, which had a longer contact time, generated greater peak inward GRF and net inward impulse than the outside limb during human curve-running. They argued that the inside limb was used primarily for generating centripetal forces, and the outside limb was used primarily for propulsion and weight support. Our study showed that the cheetah increased the duty factor only for the inside, non-lead hindlimb during curve running (Table 1). Although we did not perform GRF measurements to assess functional differences in the role of the limbs, we consider the inside, non-lead hindlimb of the cheetah to play a greater role in producing centripetal forces, and thus changing velocity heading. The other three limbs may play a role mainly in maintaining speed. The greyhound increased the duty factor for the non-lead and lead forelimbs and the lead hindlimb, suggesting that more limbs place more emphasis on changing direction rather than maintaining speed compared with cheetahs. The significant change in the hind lag between running conditions suggests that the cheetah has a greater ability to move each hindlimb individually than the greyhound. In contrast, the fore lag did not change in either species, suggesting a similar ability to move each forelimb individually.

The strategies used to deal with curve running by the cheetah may be advantageous for two reasons. Firstly, increasing the hindlimb duty factor may be more efficient than increasing forelimb duty factor because the hindlimbs support a greater proportion of body weight than the forelimbs during high-speed running (Hudson et al. 2012). Hudson et al. (2012) argued that supporting more body weight on the hindlimbs enhances grip and reduces the risk of slipping. Secondly, the inside limbs may be more tilted than the outside limbs during curve running, and thereby efficient at producing centripetal forces. During curve running, animals lean their body towards the center of the curve (Usherwood and Wilson 2005; Brocklehurst et al. 2014). As a result, the proximal joint, shoulder or hip of the inside limb is located lower than that of the outside limb. This asymmetry in the limb position may cause the differences in the coronal plane angle between the limb and the ground during stance, and thus in the effectiveness of producing centripetal and propulsive forces. The cheetah's ability to move each hindlimb individually may contribute to differing use of the inside and outside hindlimbs. Future studies are required to perform kinetic and kinematic measurements that clarify the functional roles of each limb.

In summary, our results suggest that animals do not use exactly the same strategies to deal with curve running although the effects of inter-individual variability

on results need to be assessed in the future. The cheetah may assign the roles of changing velocity and heading in the intended direction of travel to the inside, non-lead hindlimb to a greater degree than to other limbs, while the greyhound may assign these roles to multiple limbs. We expect future studies to clarify whether strategies to deal with curve running are associated with curve-running performance. This study adds to previous investigations of non-steady locomotor behavior (Biewener and Daley 2007; Daley 2016). Although most studies have restricted measurements of locomotion on a level surface in a straight line at a steady speed, animals exhibit more complex behavior in their natural environment. Turning capacity and the ability to accelerate and decelerate rapidly are as important as maximum straight-running speed for hunting success in the cheetah (Wilson et al. 2013a, 2013b). Advances in inertial measurement and data-logging technology have enabled the collection of detailed locomotion data on free-ranging animals. Experimental studies based on such free-ranging locomotion data will give us a better understanding of different ecologically important aspects of locomotor performance in animals.

References

Abourachid, A. 2003. A new way of analysing symmetrical and asymmetrical gaits in quadrupeds. Comptes Rendus Biologies 326: 625–630.

Abourachid, A., Herbin, M., Hackert, R., Maes, L. and Martin, V. 2007. Experimental study of coordination patterns during unsteady locomotion in mammals. Journal of Experimental Biology 210: 366–372.

Alexander, M. R. 2003. Principles of Animal Locomotion. Princeton University Press, Princeton, 371 pp.

Barrey, E. 2013. Biomechanics of locomotion in the athletic horse. In (Hinchcliff, K. W., Kaneps, A. J. and Geor, R. J., eds.) Equine Sports Medicine and Surgery: Basic and Clinical Sciences of the Equine Athlete, Second edition, pp. 189–211. Edinburgh, Saunders Elsevier.

Bertram, J. E. and Gutmann, A. 2009. Motions of the running horse and cheetah revisited: fundamental mechanics of the transverse and rotary gallop. Journal of The Royal Society Interface 6: 549–559.

Biancardi, C. M. and Minetti, A. E. 2012. Biomechanical determinants of transverse and rotary gallop in cursorial mammals. Journal of Experimental Biology 215: 4144–4156.

Biewener, A. A. and Daley, M. A. 2007. Unsteady locomotion: integrating muscle function with whole body dynamics and neuromuscular control. Journal of Experimental Biology 210: 2949–2960.

Biknevicius, A. R. and Reilly, S. M. 2006. Correlation of symmetrical gaits and whole body mechanics: debunking myths in locomotor biodynamics. Journal of Experimental Zoology Part A: Comparative Experimental Biology 305: 923–934.

Brocklehurst, C., Weller, R. and Pfau, T. 2014. Effect of turn direction on body lean angle in the horse in trot and canter. The Veterinary Journal 199: 258–262.

Chang, Y. H. and Kram, R. 2007. Limitations to maximum running speed on flat curves. Journal of Experimental Biology 210: 971–982.

Churchill, S. M., Trewartha, G., Bezodis, I. N. and Salo, A. I. 2016. Force production during maximal effort bend sprinting: theory vs reality. Scandinavian Journal of Medicine & Science in Sports 26: 1171–1179.

Clemente, C. J. and Wilson, R. S. 2016. Speed and maneuverability jointly determine escape success: exploring the functional bases of escape performance using simulated games. Behavioral Ecology 27: 45–54.

Daley, M. A. 2016. Non-steady locomotion. In (Bertram, J. E. A., ed.) Understanding Mammalian Locomotion: Concepts and Applications, pp. 277–306. Hoboken, Wiley-Blackwell.

Goto, M., Kawai, M., Nakata, M., Itamoto, K., Miyake, H., Ikebe, Y., Tajima, T. and Wada, N. 2013. Distribution of muscle fibers in skeletal muscles of the cheetah (*Acinonyx jubatus*). Mammalian Biology 78: 127–133.

Hayati, H., Eager, D., Jusufi, A. and Brown, T. 2017. A study of rapid tetrapod running and turning dynamics utilizing inertial measurement units in greyhound sprinting. Proceedings of the ASME 2017 International Design Engineering Technical Conferences and Computers and Information in Engineering Conference, August 6–9, Cleveland, Ohio, USA.

Hildebrand, M. 1959. Motions of the running cheetah and horse. Journal of Mammalogy 40: 481–495.

Hildebrand, M. 1977. Analysis of asymmetrical gaits. Journal of Mammalogy 58: 131–156.

Hildebrand, M. 1980. The adaptive significance of tetrapod gait selection. American Zoologist 20: 255–267.

Hudson, P. E., Corr, S. A., Payne-Davis, R. C., Clancy, S. N., Lane, E. and Wilson, A. M. 2011a. Functional anatomy of the cheetah (*Acinonyx jubatus*) hindlimb. Journal of Anatomy 218: 363–374.

Hudson, P. E., Corr, S. A., Payne-Davis, R. C., Clancy, S. N., Lane, E. and Wilson, A. M. 2011b. Functional anatomy of the cheetah (*Acinonyx jubatus*) forelimb. Journal of Anatomy 218: 375–385.

Hudson, P. E., Corr, S. A. and Wilson, A. M. 2012. High speeds galloping in the cheetah (*Acinonyx jubatus*) and the racing greyhound (*Canis familiaris*): spatio-temporal and kinetic characteristics. Journal of Experimental Biology 215: 2425–2434.

Russell, A. P. and Bryant, H. N. 2001. Claw retraction and protraction in the Carnivora: the cheetah (*Acinonyx jubatus*) as an atypical felid. Journal of Zoology, London 254: 67–76.

Sharp, N. C. C. 1997. Timed running speed of a cheetah (*Acinonyx jubatus*). Journal of Zoology, London 241: 493–494.

Stuart, D. G., Withey, T. P., Wetzel, M. C. and Goslow, G. E., Jr. 1973. Time constraints for inter-limb co-ordination in the cat during unrestrained locomotion. In (Stein, R. B., Pearson, K. G., Smith, R. S. and Redford, J. B., eds.) Control of Posture and Locomotion, pp. 537–560. Plenum Press, Kyoto.

Usherwood, J. R. and Wilson, A. M. 2005. No force limit on greyhound sprint speed. Nature 438: 753–754.

Usherwood, J. R. and Wilson, A. M. 2006. Accounting for elite indoor 200 m sprint results. Biology Letters 2: 47–50.

West, T. G., Toepfer, C. N., Woledge, R. C., Curtin, N. A., Rowlerson, A., Kalakoutis, M., Hudson, P. and Wilson, A. M. 2013. Power output of skinned skeletal muscle fibres from the cheetah (*Acinonyx jubatus*). Journal of Experimental Biology 216: 2974–2982.

Williams, D. E. and Norris, B. J. 2007. Laterality in stride pattern preferences in racehorses. Animal Behaviour 74: 941–950.

Williams, S. B., Wilson, A. M., Daynes, J., Peckham, K. and Payne, R. C. 2008a. Functional anatomy and muscle moment arms of the thoracic limb of an elite sprinting athlete: the racing greyhound (*Canis familiaris*). Journal of Anatomy 213: 373–382.

Williams, S. B., Wilson, A. M., Rhodes, L., Andrews, J. and Payne, R. C. 2008b. Functional anatomy and muscle moment arms of the pelvic limb of an elite sprinting athlete: the racing greyhound (*Canis familiaris*). Journal of Anatomy 213: 361–372.

Wilson, A. M., Lowe, J. C., Roskilly, K., Hudson, P. E., Golabek, K. A. and McNutt, J. W. 2013a. Locomotion dynamics of hunting in wild cheetahs. Nature 498: 185–189.

Wilson, J. W., Mills, M. G. L., Wilson, R. P., Peters, G., Mills, M. E. J., Speakman, J. R., Durant, S. M., Bennett, N. C., Marks, N. J. and Scantlebury, M. 2013b. Cheetahs, *Acinonyx jubatus*, balance turn capacity with pace when chasing prey. Biology Letters 9: 20130620.

Witte, T. H., Knill, K. and Wilson, A. M. 2004. Determination of peak vertical ground reaction force from duty factor in the horse (*Equus caballus*). Journal of Experimental Biology 207: 3639–3648.

Zebas, C., Gillette, R., Hailey, R., Joseph, Y. and Schoebel, T. 1991. Selected kinematic differences in the running gait of the greyhound athlete during the beginning and end of the race. In (Tant, C. L., Patterson, P. E. and York, S. L., eds.) Biomechanics in Sports IX, pp. 81–84. Ames: Iowa State University.

Figure legends

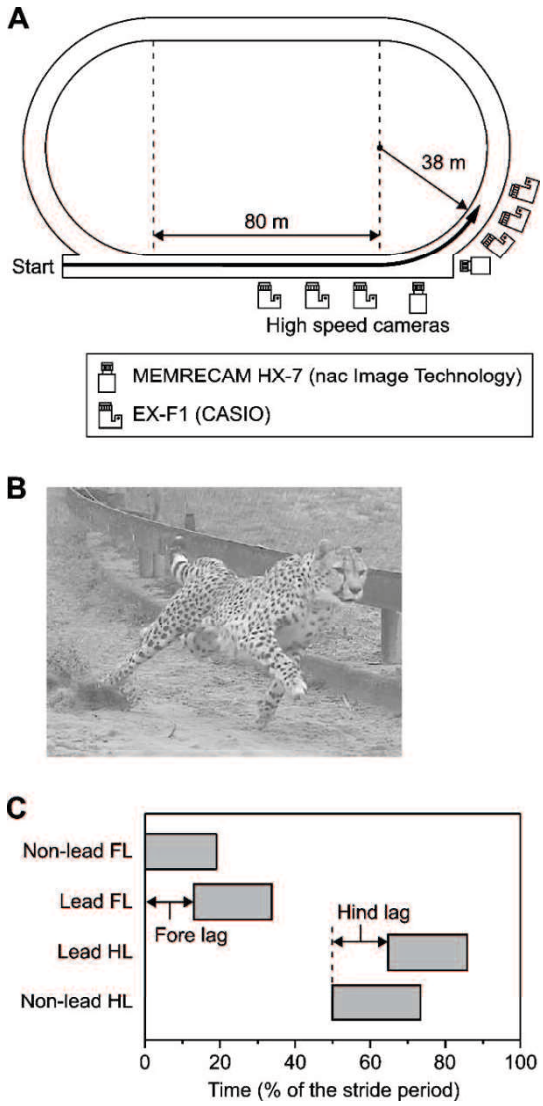

Fig. 1. A: A diagram of the track at Shanghai Wild Animal Park and the placement of eight high-speed cameras. The length of the track was 400 m. The two straight parts were each 80 m long, and the radius of the semicircular parts was 38 m. B: Photograph of a cheetah running on a curve. C: An exemplary gait diagram of the rotatory gallop. The stride period was defined as the time elapsed between two consecutive touchdowns of the non-lead forelimb and normalized to 100%. Horizontal grey bars represent the stance period. The fore lag was defined as the time between the touchdowns of the non-lead and lead forelimbs, and the hind lag was defined as the time between the touchdowns of the non-lead and lead hindlimbs. FL, forelimb; HL, hindlimb.

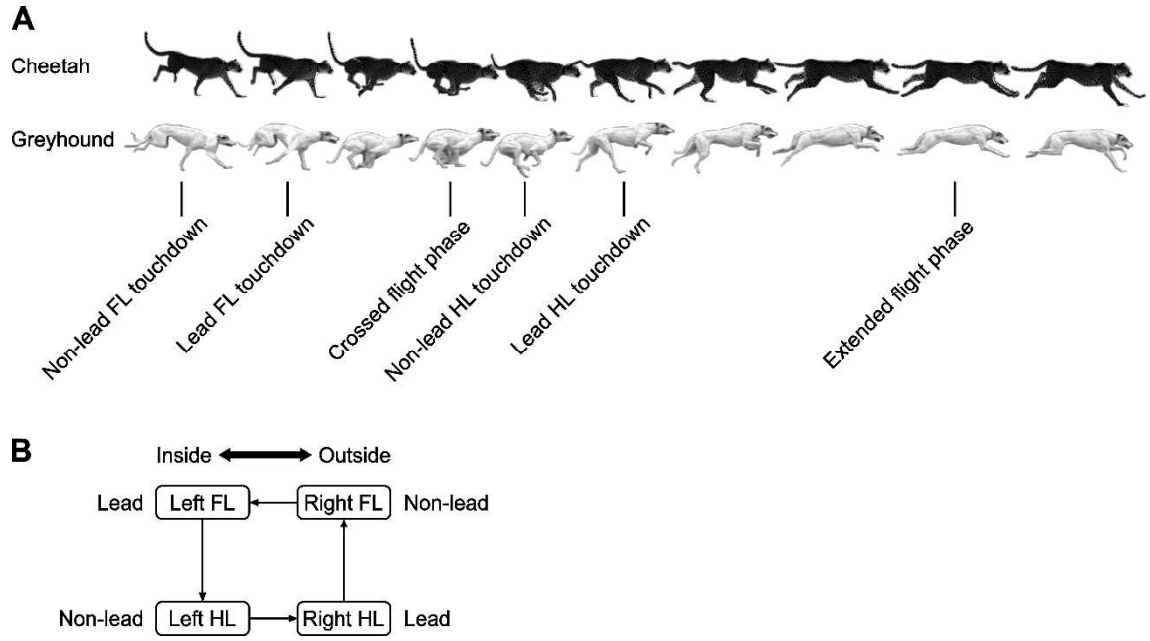

Fig. 2. A: The key points of the rotatory gallop in the cheetah and greyhound. B: The footfall pattern while running on curves in a counterclockwise direction. FL, forelimb; HL, hindlimb.

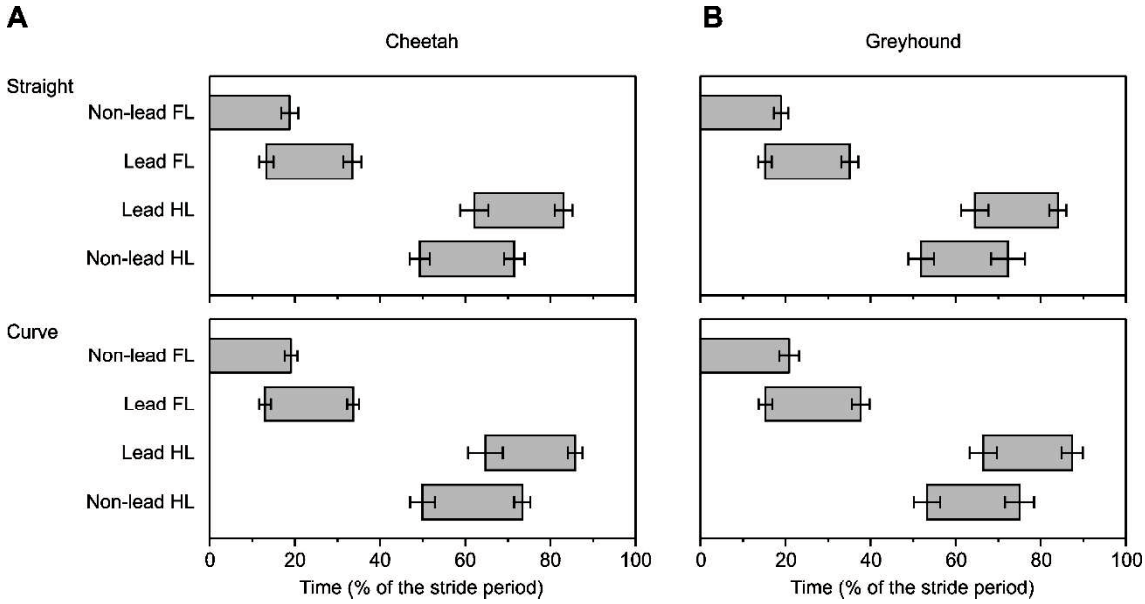

Fig. 3. Gait diagrams of straight and curve running in the cheetah (A) and greyhound (B). The stride period was normalized to 100%. Horizontal grey bars represent the mean ± SD stance period for each limb. FL, forelimb; HL, hindlimb.

Discussion on the relationship between the ability of turning in the cheetah or high speed running and muscle fiber distribution.

Goto et al.2013

Distribution of muscle fibers in skeletal muscles of the cheetah (Acinonyx jubatus, Mamm. Biol. 78, 127~133)

We examine the muscle fiber population of skeletal muscles from whole body in the cheetah (Acinonyx jubatus). In the present experiments, we showed the characteristics of fiber composition in the cheetah by comparative studies among the cheetah, domestic cat, and the beagle dog. Fiber population was determined on muscle fibers stained with monoclonal antibody to each myosin heavy chain isoform.

Histochemical analysis demonstrated that many muscles in the cheetah and domestic cat had a low percentage of Type I fibers and a high percentage of Type IIx fibers, while those in the beagle dog showed a high percentage of Type IIa. The hindlimb muscles in the cheetah had a higher percentage of Type II (Type IIa + IIx) fiber than the forelimb muscles. This fact suggests that the propulsive role of the hindlimb is greater than the forelimb in the cheetah. The longissimus in the cheetah had a high percentage of Type IIx fibers over a wide range from the thoracic to lumbar parts,

while the population of muscle fibers in this muscle was different depending on the parts in the domestic cat and beagle dog. This indicates that the cheetah can produce a strong and quick extension of the spinal column and increase its stiffness during locomotion. Furthermore, we found the notable difference of muscle fiber type population between flexors and extensors of digits in the cheetah. The present experiments show the characteristics of muscle fibers in the cheetah, corresponded to its ability to perform high-speed running.

Summary-1

The characteristics of muscle fiber distribution in cheetah's muscles (comparison with cat and dogs) shown in the paper by Goto et al. are 1. high content of fast muscle fiber distribution in m. erector spine, 2. a remarkable difference of muscle fibers distribution between flexors and extensors controlling finger motion. In our paper, the cheetah can run thorough the curve without changing the running speed by changing the timing of landing of limbs. For running in the corner, it is necessary to control the quickly motion control of toe and increasing stiffness of spine to stabilize the leg motion. Muscle fiber distribution in cheetah's muscles not only enable high-speed running, but also allows curving or changing running direction at high speed. Our

results are closely related to the results of studies on muscle fiber distribution in cheetah.

In the cheetah, a closely relationship between locomotion and muscle fiber distribution, which is the purpose of research of the doctoral course was shown.

Studies of muscle fiber distribution in mole.

Characteristics of muscle fiber type distribution in moles

Introduction

Moles spend most of their lives underground. The subterranean habitat provides protection from predators and access to food (Nevo, 1979). As moles build narrow burrows underground (Mellanby, 1971; Gorman and Stone, 1990), they do not have to support their body weight with their limbs and rarely need to maintain body equilibrium like terrestrial animals. Moles possess a suite of specialized adaptations to subterranean life. Their body is cylindrically shaped (Nevo, 1979), and their broad hands contain five strong claws with the palm turned permanently outward (Yalden, 1966). Although these observations suggest that moles are relatively slow and sluggish, they are also powerful diggers capable of rapid bursts of forelimb activity while excavating new burrows. Obtaining sufficient oxygen for aerobic ATP production during these periods may be compromised as oxygen levels tend to be lower underground (Nevo, 1979). Thus, the unusual lifestyle of moles together with the physical characteristics of their subterranean habitat are expected to have affected their musculature system.

Moles belong to the order Soricomorpha. This taxon includes moles, desmans, and shrews. Two groups of moles, the tribes Talpini and Scalopini, exhibit specialized

adaptations to subterranean life (Bannikova et al., 2015). Shrew-moles are generally considered to be “moles”, but they are not strictly fossorial. To avoid confusion, we hereafter refer to strictly fossorial moles as true moles.

Mammalian skeletal muscles are commonly composed of muscle fibers with differing contractile and metabolic characteristics. Many studies have demonstrated a close relationship between the fiber type distribution and the function of the muscle, and have suggested that fiber type distribution correlates well with the locomotion of the animal (Ariano et al., 1973; Johnson et al., 1973; Essén et al., 1975; Hintz et al., 1980; Reichmann and Pette, 1982; Suzuki et al., 1983; Van Den Hoven et al., 1985; Sugiura and Murakami, 1990; Dearolf et al., 2000; Schmidt and Schilling, 2007; Toniolo et al., 2007; Cotten et al., 2008; Kawai et al., 2009; Smerdu et al., 2009; Kohn et al., 2011; Williams et al., 2011; Curry et al., 2012; Goto et al., 2013a, 2013b; Hazimihalis et al., 2013; Kielhorn et al., 2013). For example, muscles of the African elephant (*Loxodonta africana*) have a relatively high percentage of Type I fibers (Goto et al., 2013a). Type I fibers shorten slowly and are highly resistant to fatigue compared with Type II fibers. Therefore, the high percentage of Type I fibers in muscles allows elephants to support and move their massive body (Goto et al., 2013a). In contrast, many muscles of the cheetah (*Acinonyx jubatus*) are composed of a high percentage of fast Type IIx fibers,

which are suited to high-speed running (Hyatt et al., 2010; Goto et al., 2013b). A few studies have reported the muscle fiber type distribution in Soricomorpha, including the house shrew (*Suncus murinus*) by Suzuki (1990), the common shrew (*Sorex araneus*) by Savolainen and Vornanen (1995), and the Etruscan shrew (*Suncus etruscus*) and common European white-toothed shrew (*Crocidura russula*) by Peters et al. (1999). In these species, Type I fibers were absent in all the muscles examined. However, little is known about the muscle fiber type distribution in true moles.

To clarify the contractile function of skeletal muscles in true moles, we compared the muscle fiber type distribution in two true-mole species with that in four other Soricomorpha species with different locomotive habits (Table 1). Multispecies comparisons within a phylogenetically narrow lineage help to distinguish an adaptation from a phylogenetic effect in which different species are similar due to traits inherited from a common ancestor (Losos and Miles, 1994). The true moles studied included the large Japanese mole (*Mogera wogura*) and the lesser Japanese mole (*Mogera imaizumii*). The large Japanese mole is commonly considered to be larger than the lesser Japanese mole in overall size (Abe, 2001; Ohdachi et al., 2015), and they both belong to the tribe Talpini in the family Talpidae. These true mole species were compared with the Japanese shrew-mole (*Urotrichus talpoides*), house shrew, Japanese white-toothed

shrew (*Crocidura russula*), and the Japanese water shrew (*Chimarrogale platycephala*). The Japanese shrew-mole is semi-fossorial and a member of the family Talpidae, similar with the large Japanese mole and lesser Japanese mole. The remaining three species belong to the family Soricidae. The house shrew and the Japanese white-toothed shrew are terrestrial. The Japanese water shrew is semi-aquatic and dives into streams to forage. This Soricomorpha species exhibits adaptations for its aquatic lifestyle (Ohdachi et al., 2015).

We assessed the muscle fiber type using immunohistochemical staining and/or sodium dodecyl sulfate-polyacrylamide gel electrophoresis (SDS-PAGE). For immunohistochemistry, we used three primary monoclonal antibodies: anti-fast myosin, SC-71, and BF-35. These are commonly used antibodies, and anti-fast myosin and SC-71 successfully distinguished different fiber types in muscles of the Thoroughbred horse, African elephant, cheetah, dog, and cat in our previous studies (Kawai et al., 2009; Goto et al., 2013a, 2013b). However, the specificity of the antibodies has not yet been tested in Soricomorpha. Thus, we performed SDS-PAGE in addition to immunohistochemistry to prevent incorrect identification of fiber types. We did not carry out SDS-PAGE fiber typing for the house shrew. We tested the specificity of the antibodies in the house shrew by comparing our results with those of Suzuki (1990).

We tested two hypotheses regarding muscle fiber type distribution in true moles. First, we hypothesized that the contractile function of muscles in true moles is suited to their unusual lifestyle in the subterranean environment. Therefore, we predicted that true mole muscles have a characteristic fiber type distribution compared with the other Soricomorpha species. Second, we hypothesized that the forelimb muscles of true-moles are adapted to powerful digging with rapid bursts of forelimb activity. This hypothesis is based on the observations that only the forelimbs are used in digging (Skoczeń, 1958; Mellanby, 1971) and that the hind limb displays less morphological modification for this behavior (Mellanby, 1971). We expected the forelimb muscles to be composed of a higher percentage of anaerobic Type IIb fibers, which may be beneficial for digging, than muscles in other anatomical regions.

Materials and methodes

Animals and Muscles

Two large Japanese moles, one lesser Japanese mole, two Japanese shrew-moles, two house shrews, one Japanese white-toothed shrew, and one Japanese water shrew were used (Table 1). The large Japanese moles, lesser Japanese mole, Japanese shrew-moles, Japanese white-toothed shrew, and Japanese water shrew were caught in

the vicinity of Yamaguchi City (Yamaguchi Prefecture, Japan) and the Tsukuba Botanical Garden at the National Museum of Nature and Science (Ibaraki Prefecture, Japan). The house shrews were provided by Okayama University of Science (Okayama Prefecture, Japan). All experimental procedures were approved by the Institutional Animal Care and Use Committee at Yamaguchi University.

Fiber type distribution was characterized for up to 38 muscles in a single species (Table 1 and Fig. 1). The muscles studied included 12 forelimb muscles, 16 hind limb muscles, nine trunk muscles, and the diaphragm. For the lesser Japanese mole, a 13-muscles subset was examined. For the Japanese shrew-mole, the flexor digitorum profundus of the forelimb and extensor digitorum communis were not examined. For the Japanese water shrew, the diaphragm was not examined.

All animals were anesthetized with sodium pentobarbital (35–55 mg/kg, intraperitoneal). For each muscle, the whole muscle was dissected free. The muscles were frozen in liquid nitrogen and stored at −80°C. After dissection, animals were sacrificed by sodium pentobarbital overdose (95 mg/kg, intraperitoneal).

Immunohistochemistry

Four to eight 10-μm thick cross-sections were cut at the mid-belly portion of each muscle using a cryostat (Leica, Nusslock, Germany) at −20°C. The sections were thawed to room temperature and then preincubated with goat normal serum in 0.2 M phosphate buffer (pH 7.6) at 25°C for 10 min. Afterwards, the three primary monoclonal antibodies, anti-fast myosin (M4276; Sigma-Aldrich, St. Louis, MO), SC-71 (Developmental Studies Hybridoma Bank, Iowa City, IA), and BF-35 (Developmental Studies Hybridoma Bank, Iowa City, IA), were applied. Anti-fast myosin reacts specifically with myosin heavy chain (MHC) II, SC-71 reacts specifically with MHC IIa, and BF-35 reacts specifically with MHC I, IIa, and IIb. The sections were incubated at 25°C for 180 min, washed with phosphate buffer, and then incubated for a further 180 min at 25°C with a secondary antibody (goat anti-mouse IgG) conjugated with horseradish peroxidase (Bio-Rad, Hercules, CA). The sections were then washed again with phosphate buffer. The secondary antibodies were reacted with diaminobenzidine tetrahydrochloride as a chromogen to visualize the conjugated peroxidase (Kawai et al., 2009). Micrographs of the stained muscle fibers were obtained using a microscope (Nikon E600, Tokyo, Japan) equipped with an image-processing system (Nikon DS-U1, Tokyo, Japan).

Muscle fibers were classified as Type I, IIa, IIx, or IIb using immunohistochemically-stained micrographs. Type I fibers were stained weakly with anti-fast myosin and SC-71. Type IIa fibers were stained strongly with anti-fast myosin, SC-71, and BF-35. Type IIx fibers were stained strongly with anti-fast myosin, but weakly with SC-71 and BF-35. Type IIb fibers were stained strongly with anti-fast myosin and BF-35, but weakly with SC-71. In addition to these "pure" fiber types, hybrid Type IIa/x fibers were stained strongly with anti-fast myosin and SC-71, but weakly with BF-35. We designated Type IIa/x fibers as Type IIx fibers. The percentage distribution of individual fiber types was calculated based on approximately 500 fibers for each muscle. To do this, five regions containing more than 100 fibers each were selected on the micrographs. One region was at the center of the micrographs, and the remaining four regions were above, below, and to the left and right. We did not determine the fiber type for all muscle fibers in a muscle. This selective process was required to examine muscles over the entire body in many species, and is not uncommon in studies on muscle fiber type distribution (Kawai et al., 2009; Tirrell et al., 2012; Goto et al., 2013a, 2013b; O'Neill et al., 2017). Furthermore, fiber cross-sectional areas (CSA) were measured for at least 25 fibers of each type.

Electrophoresis

For some of the muscles that were subjected to immunohistochemistry, fiber type distribution was also characterized using SDS-PAGE. This analysis was performed for the following muscles: the vastus lateralis, deltoid, medial head of triceps brachii, serratus abdominis, infraspinatus, long head of triceps brachii, biceps brachii, extensor digitorum communis, trapezius, pectoralis superficialis, diaphragm, biceps femoris, gastrocnemius lateralis, and flexor digitorum profundus in the large Japanese mole; the latissimus dorsi, trapezius, pectoralis superficialis, gluteus medius in the lesser Japanese mole; and the vastus lateralis and deltoid in the Japanese shrew-mole, Japanese white-toothed shrew, and Japanese water shrew. The vastus lateralis of the laboratory rat was used as MHC isoform references as this muscle is composed of Type I, IIa, IIx, and IIb fibers (Delp and Duan, 1996).

The mid-belly portion of each muscle was homogenized in SDS sample buffer containing 30% (v/v) glycerol, 5% (v/v) β-mercaptoethanol, 2.3% (w/v) SDS, 62.5 mM Tris-HCl (pH 6.8), and 0.05 (w/v) bromophenol blue (1:40 wt/vol). The homogenate was incubated for 10 min at 60°C, and further diluted 1:10 (v/v) with SDS sample buffer. A 7.5-µl sample of the homogenate was electrophoresed according to a modified version of the technique used by Sugiura and Murakami (1990). In brief, the separating

gel contained 8% (w/v) acrylamide, 33.3% (v/v) glycerol, 0.375 M Tris-HCl (pH 8.8), 0.1% (w/v) SDS, 0.0375 (w/v) ammonium persulphate, and 0.0008 (v/v) TEMED. The stacking gel contained 4% (w/v) acrylamide, 33.3% (v/v) glycerol, 0.125 M Tris-HCl (pH 6.8), 0.1% (w/v) SDS, 0.0375 (w/v) ammonium persulphate, and 0.0008 (v/v) TEMED. Electrophoresis began at 50 V until the tracking dye completely entered the separating gel, at which the voltage was increased to 150 V for ~18 h at 8°C. The gels were then stained using EzStain AQUA (ATTO Corporation, Tokyo).

To calculate the percentage distribution of individual MHC isoforms, densitometric scans of the gels and the area under each densitometric peak were measured using ImageJ software (National Institutes of Health, Bethesda, MD).

Statistical Analysis

The level of significance was set at $\alpha = 0.05$. To evaluate differences in CSA between muscle fiber types, one-way ANOVA and post-hoc multiple comparisons were used for a muscle that comprised three or more fiber types, and the *t* test was used for muscles comprising two fiber types.

Results

Fiber Type Distribution by Immunohistochemistry

Almost all fibers in the muscles of the large Japanese moles and lesser Japanese mole, or true moles, were stained strongly with all three antibodies used (Fig. 2). In the muscles of the other Soricomorpha species, almost all fibers were stained strongly with anti-fast myosin, while reactivity to SC-71 and BF-35 varied among fibers.

The true mole muscles were composed almost exclusively of Type IIa fibers (Fig. 1). Only in the subscapularis, tibialis anterior, and pectoralis superficialis of the large Japanese moles were Type IIx fibers observed in addition to Type IIa fibers (Fig. 1A). Type I and Type IIb fibers were absent. Furthermore, the fiber type distribution was similar in the forelimb, hind limb, and trunk (Table 2).

The muscles of the Japanese shrew-mole were composed of three subtypes of Type II fibers (Fig. 3). Type I fibers were absent. Only Type IIa fibers were present in the biceps femoris and tibialis anterior, and there were only Type IIx fibers in the lateral head of the triceps brachii and the vastus lateralis. Two subtypes of Type II fibers were present in nine muscles. The medial head of the triceps brachii, gluteus medius, trapezius, and longissimus thoracis were composed of Type IIa and IIx fibers. The semimembranosus, gastrocnemius lateralis, extensor digitorum longus, and diaphragm

were composed of Type IIa and IIb fibers. The longissimus lumborum was composed of Type IIx and IIb fibers. The remaining muscles were composed of all three Type II fiber subtypes.

The muscles of the house shrew were composed of Type IIa and Type IIx fibers (Figs. 2 and 4). Type I and IIb fibers were absent. There were only Type IIa fibers in the flexor digitorum profundus of the forelimb, iliacus, and pectoralis profundus.

The muscles of the Japanese white-toothed shrew were composed of three subtypes of Type II fibers (Fig. 5). Type I fibers were not observed. Generally, the percentage of Type IIa and IIb fibers was higher than that of Type IIx fibers. A predominance of Type IIb fibers was observed in most muscles. A predominance of Type IIa fibers was observed in seven muscles: the flexor digitorum profundus of the forelimb, vastus medialis, gastrocnemius lateralis, trapezius, serratus abdominis, obliquus externus, and the diaphragm. Only Type IIa fibers were observed in the trapezius.

The muscles of the Japanese water shrew were composed of three subtypes of Type II fibers (Figs. 2 and 6). Type I fibers were absent, as in the other Soricomorpha species studied. Generally, the muscles of the Japanese water shrew contained higher percentages of Type IIa and IIx fibers than those of the Japanese white-toothed shrew.

Type IIb fibers were not observed in 11 muscles: the brachialis, flexor digitorum profundus of the forelimb, psoas major, iliacus, rectus femoris, vastus medialis, flexor digitorum profundus of the hind limb, obliquus externus, rectus abdominis, longissimus thoracis, and the longissimus lumborum.

Fiber Cross-Sectional Area

The CSA of Type IIa fibers varied between 559 and 1674 μm^2 in the large Japanese mole and between 596 and 1169 μm^2 in the lesser Japanese mole (Fig. 7). For the Japanese shrew-mole, Japanese white-toothed shrew, and Japanese water shrew, the CSA of Type IIb fibers were larger than that of Type IIa and Type IIx fibers. For the house shrew, the CSA of Type IIx fibers was significantly larger than that of Type IIa fibers in each anatomical region.

Fiber Type Distribution by Electrophoresis

Gel electrophoresis revealed that MHC I isoforms were negligible in all muscles examined of the large Japanese mole, lesser Japanese mole, Japanese shrew-mole, Japanese white-toothed shrew, and Japanese water shrew (Fig. 8). MHC IIb isoforms were clearly observed in the vastus lateralis and/or deltoid in the Japanese shrew-mole,

Japanese white-toothed shrew, and Japanese water shrew (Fig. 8A). In contrast, the true mole muscles contained mainly MHC IIa and IIx isoforms and, a very small percentage (<5.0%) of MHC IIb isoforms (Fig. 8B). Furthermore, the forelimb muscles did not contain a higher percentage of Type IIb fibers than those of the hindlimb and trunk (Table 2).

Discussion

We investigated the muscle fiber type distribution in six Soricomorpha species with different locomotive habits to clarify the contractile function of skeletal muscles in strictly fossorial moles. Most of the data presented here are new, but the muscle fiber types in hind limb muscles of the house shrew were examined by myosin ATPase staining by Suzuki (1990). Before discussing the results and their implications, it is important to note differences between our results and those of Suzuki (1990). The study by Suzuki (1990) demonstrated that hind limb muscles of the house shrew were composed of Type IIa, intermediate, and Type IIb fibers, with Type I fibers being absent. Immunohistochemistry performed in our study revealed that the hind limb muscles were composed of Type IIa and IIx fibers, with Type I and IIb fibers being absent (Fig. 4). The cause of this discrepancy is unknown, and may be a result of different

characterization methods or lack of reactivity of MHC IIb isoforms in house shrew muscles with the antibodies used. The most valid interpretation of our results is that they extend Suzuki's findings (1990) by confirming that Type I fibers are absent in muscles throughout the body in the house shrew.

It is also necessary to mention two limitations of this study. First, the sample size was small for each species. One or two animals each were used in this study. Second, the muscle fiber type distribution in a single muscle was determined based on ~500 fibers, but not on all fibers. These limitations prevent us from discussing intraspecific variability or regional differences within a muscle. However, the focus of this study was on identifying patterns common to muscles over the entire body of true moles. The true mole provides a good model for studying adaptation because of its unusual lifestyle underground. Although characterization of fiber type distribution based on all the fibers that compose a muscle in many individuals may be preferable compared to our approach (Delp and Duan, 1996), we made attempts to reduce the influence of muscle fiber regionalization on results by selecting the fibers in five regions evenly distributed over the muscle cross-section.

We assessed fiber types using both immunohistochemistry and SDS-PAGE for some muscles of the large Japanese mole, lesser Japanese mole, Japanese shrew-mole,

Japanese white-toothed shrew, and Japanese water shrew. The two methods of typing did not give identical results. Of note, immunohistochemistry demonstrated that muscles of true moles were composed of Type IIa fibers alone (Figs. 1 and 2), but SDS-PAGE indicated that they were composed of Type IIa and Type IIx fibers (Fig. 8). We used the mid-belly portion of the muscle for both immunohistochemistry and SDS-PAGE. Therefore, it is unlikely that the differences in results between the two methods reflect muscle fiber regionalization alone. Rather, the results suggest that SC-71 and BF-35 may cross-react with IIx fibers in the true mole muscles. However, these antibodies did not react with IIx fibers in the subscapularis, tibialis anterior, and pectoralis superficialis of the large Japanese moles. A possible explanation for this discrepancy is that hybrid fibers, including IIa/x and IIx/b fibers, are present in the true mole muscles and differ in reactivity to SC-71 and BF-35 compared to IIx fibers.

Accordingly, the discussion below is based on three consistent results. First, Type I fibers were almost entirely absent in all the muscles examined of the six Soricomorpha species. Second, neither Type IIb fibers nor Type I fibers were observed in true mole muscles. Last, in the true moles, the forelimb muscles did not contain a higher percentage of Type IIb fibers than those of the hind limbs and trunk.

This study furthers previous reports that Type I fibers are absent in the muscles of Soricomorpha species. The absence of Type I fibers was confirmed in nine species with different locomotive habits: the large Japanese mole (Fig. 1A), lesser Japanese mole (Fig. 1B), Japanese shrew-mole (Fig. 3), house shrew (Suzuki, 1990; Fig. 4), Etruscan shrew (Peters et al., 1999), Japanese white-toothed shrew (Fig. 5), common European white-toothed shrew (Peters et al., 1999), common shrew (Savolainen and Vornanen, 1995), and Japanese water shrew (Fig. 6). This muscle fiber type composition in Soricomorpha is unique among mammals. Type I fibers are observed in muscles of a variety of animals spanning a wide range of body sizes (O'Neill et al., 2017 and literature therein), including laboratory mice (body weight, ~20 g; Wang and Kernall, 2001; Glaser et al., 2009), laboratory rats (150–429 g; Talmadge et al., 1999; Delp and Duan, 1996; Kohn and Myburgh, 2007), common tree shrews (*Tupaia glis*; 133–214 g), and Senegal bushbabies (*Galago senegalensis*; 174–270 g; Sickles and Pinkstaff, 1981). Therefore, it is unlikely that the small body size of Soricomorpha or locomotor adaptations alone determine the composition of Type I fibers in their muscles (Suzuki, 1990). The absence of Type I fibers may be due to phylogenetic effects.

Muscle Fiber Type Distribution in Strictly Fossorial Moles

We found that the muscles of true moles were unique in that they contained neither Type IIb fibers nor Type I fibers (Figs. 1, 2, and 8). In contrast, the muscles of the semi-fossorial, terrestrial, and semi-aquatic Soricomorpha species contained all three subtypes of Type II fibers, although fiber type distribution in the house shrew needs to be investigated further. These results agree with our first hypothesis that the contractile function of muscles in true moles is related to subterranean environments, which are structurally simple compared with terrestrial habitats (Nevo, 1979). In subterranean environments, there is no need to support the body weight with limbs, or to move at high speeds to pursue prey or to escape from predators. On the other hand, terrestrial animals must maintain body equilibrium with limbs to prevent falling, and maximum speed and maneuverability are key factors that determine success in hunting prey and escaping from predators. Given these differences between habitats, the homogenous fiber type distribution in muscles of the true mole is considered to be well suited to structurally simple subterranean environments.

Contrary to our second hypothesis, the forelimb muscles of true moles were not composed of a higher percentage of Type IIb fibers than those of the hind limbs and trunk (Table 2). This result is unexpected given the use of the forelimbs for powerful

digging (Skoczeń, 1958; Mellanby, 1971) and lower oxygen levels underground (Nevo, 1979). In addition, the percentage of each fiber type was similar among different anatomical regions. These results suggest that fiber type distribution in muscles over the entire body of the true mole strongly reflects adaptation to subterranean environments rather than distinct functions assigned to each anatomical region.

Our results allow us to speculate on motor unit recruitment in the true mole. According to Henneman's size principle (Henneman and Olson, 1965), motor units are orderly recruited from smallest to largest. This is because small units are composed of small-diameter motor nerves with high excitability. In contrast, large units are composed of large-diameter motor nerves with low excitability. Furthermore, muscle fiber type composition in a motor unit is generally uniform, and motor unit size is correlated with muscle fiber type (Biewener, 2003). Small units contain slow fibers, whereas large units contain fast fibers. Thus, Henneman's size principle also implies that muscle fibers are orderly recruited from slowest to fastest. The homogenous fiber type distribution in true mole muscles suggests that the size and excitability of motor units are less variable, limiting fine adjustment of the level of force output. To examine whether control of the force output of muscles in the true mole is simple, we are now

evaluating a nerve-muscle preparation by combining electrical stimulation and twitch tension recording.

References

Abe A. 2001. Soil hardness, a factor affecting the range expansion of *Mogera wogura* in Japan. Mammal Study 26:45–52.

Ariano MA, Armstrong RB, Edgerton VR. 1973. Hindlimb muscle fiber populations of five mammals. J Histochem Cytochem 21:51–55.

Bannikova AA, Zemlemerova ED, Lebedev VS, Aleksandrov DY, Fang Y, Sheftel BI. 2015. Phylogenetic position of the Gansu mole *Scapanulus oweni* Thomas, 1912 and the relationships between strictly fossorial tribes of the family Talpidae. Doklady Biol Sci 464:230–234.

Biewener AA. 2003. Animal locomotion. Oxford: Oxford University Press.

Cotten PB, Piscitelli MA, McLellan WA, Rommel SA, Dearolf JL, Pabst DA. 2008. The gross morphology and histochemistry of respiratory muscles in bottlenose dolphins, *Tursiops truncatus*. J Morphol 269:1520–1538.

Curry JW, Hohl R, Noakes TD, Kohn TA. 2012. High oxidative capacity and type IIx fibre content in springbok and fallow deer skeletal muscle suggest fast sprinters with a resistance to fatigue. J Exp Biol 215:3997–4005.

Dearolf JL, McLellan WA, Dillaman RM, Frierson D, Pabst DA. 2000. Precocial development of axial locomotor muscle in bottlenose dolphins (*Tursiops truncatus*). J Morphol 244:203–215.

Delp MD, Duan C. 1996. Composition and size of type I, IIA, IID/X, and IIB fibers and citrate synthase activity of rat muscle. J Appl Physiol 80:261–270.

Essén B, Jansson E, Henriksson J, Taylor AW, Saltin B. 1975. Metabolic characteristics of fibre types in human skeletal muscle. Acta Physiol Scand 95:153–65.

Glaser BW, You G, Zhang M, Medler S. 2009. Relative proportions of hybrid fibres are unaffected by 6 weeks of running exercise in mouse skeletal muscles. Exp Physiol 95:211–221.

Goto M, Itamoto K, Tani Y, Miyata H, Kihara I, Mori F, Tajima T, Wada N. 2013a. Distribution of muscle fibers in skeletal muscles of the African elephant (*Loxodonta africana africana*). *Mammal Study* 38:135–140.

Goto M, Kawai M, Nakata M, Itamoto K, Miyata H, Ikebe Y, Tajima T, Wada N. 2013b. Distribution of muscle fibers in skeletal muscles of the cheetah (*Acinonyx jubatus*). *Mamm Biol* 78:127–133.

Gorman ML, Stone RD. 1990. The natural history of moles. Ithaca: Comstock Publishing Associates.

Hazimihalis PJ, Gorvet MA, Butcher MT. 2013. Myosin isoform fiber type and fiber size in the tail of the Virginia opossum (*Didelphis virginiana*). Anat Rec 296:96–107.

Henneman E, Olson CB. 1965. Relations between structure and function in the design of skeletal muscles. J Neurophysiol 28:581–598.

Hintz CS, Lowry CV, Kaiser KK, McKee D, Lowry OH. 1980. Enzyme levels in individual rat muscle fibers. Am J Physiol Cell Physiol 239:C58–C65.

Hyatt JPK, Roy RR, Rugg S, Talmadge RJ. 2010. Myosin heavy chain composition of tiger (*Panthera tigris*) and cheetah (*Acinonyx jubatus*) hindlimb muscles. J Exp Zool 313A:45–57.

Johnson MA, Polgar J, Weightman D, Appleton D. 1973. Data on the distribution of fibre types in thirty-six human muscles. An autopsy study. J Neurol Sci 18:111–129.

Kawai M, Minami Y, Sayama Y, Kuwano A, Hiraga A, Miyata H. 2009. Muscle fiber population and biochemical properties of whole body muscles in Thoroughbred horses. Anat Rec 292:1663–1669.

Kielhorn CE, Dillaman RM, Kinsey ST, McLellan WA, Gay DM, Dearolf JL, Pabst DA. 2013. Locomotor muscle profile of a deep (*Kogia breviceps*) versus shallow (*Tursiops truncatus*) diving cetacean. J Morphol 274:663–675.

Kohn TA, Curry JW, Noakes TD. 2011. Black wildebeest skeletal muscle exhibits high oxidative capacity and a high proportion of type IIx fibres. J Exp Biol 214:4041–4047.

Kohn TA, Myburgh KH. 2007. Regional specialization of rat quadriceps myosin heavy chain isoforms occurring in distal to proximal parts of middle and deep regions is not mirrored by citrate synthase activity. J Anat 210:8–18.

Losos JB, Miles DB. 1994. Adaptation, constraint, and the comparative method: phylogenetic issues and methods. In: Wainwright PC, Reilly S, editors. Ecological morphology: integrative organismal biology. Chicago: University of Chicago Press. p. 60–98.

Mellanby K. 1971. The mole. New York: Taplinger Publishing Company.

Nevo E. 1979. Adaptive convergence and divergence of subterranean mammals. Annu Rev Ecol Syst 10:269–308.

Ohdachi SD, Ishibashi Y, Iwasa MA, Fukui D, Saitoh T, editors. 2015. The wild mammals of Japan. 2nd ed. Kyoto: Shoukadoh Book Sellers.

O'Neill MC, Umberger BR, Holowka NB, Larson SG, Reiser PJ. 2017. Chimpanzee super strength and human skeletal muscle evolution. Proc Natl Acad Sci U S A 114:7343–7348.

Peters T, Kubis HP, Wetzel P, Sender S, Asmussen G, Fons R, Jürgens KD. 1999. Contraction parameters, myosin composition and metabolic enzymes of the skeletal muscles of the etruscan shrew *Suncus etruscus* and of the common European white-toothed shrew *Crocidura russula* (Insectivora: soricidae). J Exp Biol 202:2461–2473.

Reichmann H, Pette D. 1982. A comparative microphotometric study of succinate dehydrogenase activity levels in type I, IIA and IIB fibres of mammalian and human muscles. Histochemistry 74:27–41.

Savolainen J, Vornanen M. 1995. Fiber types and myosin heavy chain composition in muscles of common shrew (*Sorex araneus*). J Exp Zool 271:27–35.

Schmidt M, Schilling N. 2007. Fiber type distribution in the shoulder muscles of the tree shrew, the cotton-top tamarin, and the squirrel monkey related to shoulder movements and forelimb loading. J Hum Evol 52:401–419.

Skoczeń S. 1958. Tunnel digging by the mole (*Talpa europaea* Linne). Acta Theoriol 2:235–249.

Sickles DW, Pinkstaff CA. 1981. Comparative histochemical study of prosimian primate hindlimb muscles. I. Muscle fiber types. Am J Anat 160:175–186.

Smerdu V, Cehovin T, Strbenc M, Fazarinc G. 2009. Enzyme- and immunohistochemical aspects of skeletal muscle fibers in brown bear (*Ursus arctos*). J Morphol 270:154–161.

Sugiura T, Murakami N. 1990. Separation of myosin heavy chain isoforms in rat skeletal muscles by gradient sodium dodecyl sulfate-polyacrylamide gel electrophoresis. Biomed Res 11:87–91.

Suzuki A. 1990. Composition of myofiber types in limb muscles of the house shrew (*Suncus murinus*): lack of type I myofibers. Anat Rec 228:23–30.

Suzuki A, Tsuchiya T, Takahashi Y, Tamate H. 1983. Histochemical properties of myofibers in longissimus muscle of common dolphins (*Delphinus delphis*). Acta Histochem Cytochem 16:223–231.

Talmadge RJ, Roy RR, Edgerton VR. 1999. Persistence of hybrid fibers in rat soleus after spinal cord transection. Anat Rec 255:188–201.

Tirrell TF, Cook MS, Carr JA, Lin E, Ward SR, Lieber RL. 2012. Human skeletal muscle biochemical diversity. J Exp Biol 215:2551–2559.

Toniolo L, Maccatrozzo L, Patruno M, Pavan E, Caliaro F, Rossi R, Rinaldi C, Canepari M, Reggiani C, Mascarello F. 2007. Fiber types in canine muscles: myosin isoform expression and functional characterization. Am J Physiol Cell Physiol 292:C1915–C1926.

Van Den Hoven R, Wensing T, Breukink HJ, Meijer AE, Kruip TA. 1985. Variation of fiber types in the triceps brachii, longissimus dorsi, gluteus medius, and biceps femoris of horses. Am J Vet Res 4: 939–941.

Wang LC, Kernell D. 2001. Fibre type regionalisation in lower hindlimb muscles of rabbit, rat and mouse: a comparative study. J Anat 199:631–643.

Williams TM, Noren SR, Glenn M. 2011. Extreme physiological adaptations as predictors of climate-change sensitivity in the narwhal, *Monodon monoceros*. Mar Mammal Sci 27:334–349.

Wilson DE, Reeder DM, editors. 2005. Mammal Species of the World: A Taxonomic and Geographic Reference. 3rd ed. Baltimore: Johns Hopkins University Press.

Yalden DW. 1966. The anatomy of mole locomotion. J Zool 149:55–64.

Figure legends

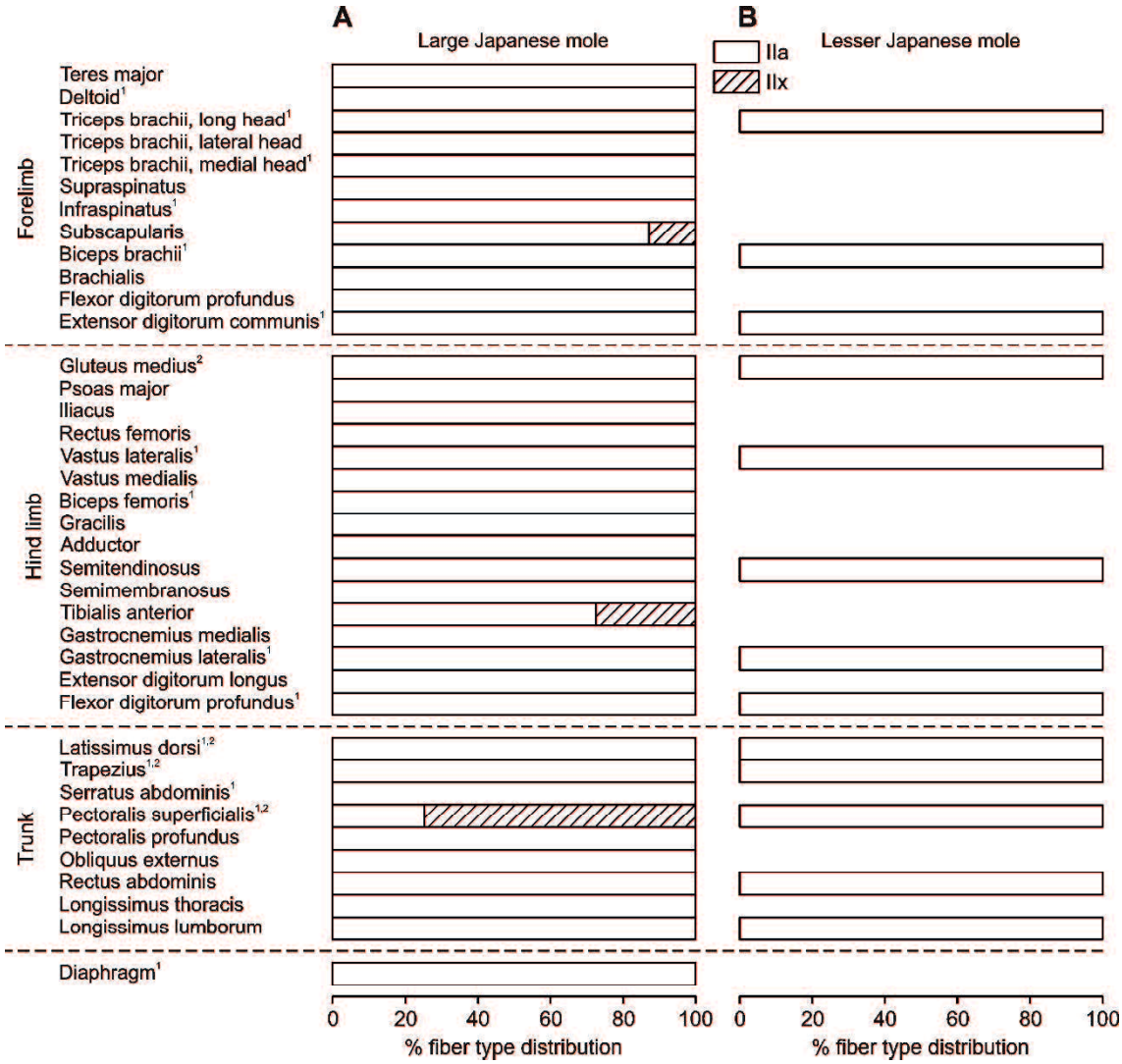

Fig. 1. Fiber type distribution percentage measured immunohistochemically in (A) 38 muscles of the large Japanese mole (*Mogera wogura*) and (B) 13 muscles of the lesser Japanese mole (*Mogera imaizumii*). For the muscles marked with superscript numbers, myosin heavy chain (MHC) distribution was further characterized electrophoretically for 1 large Japanese mole and 2 lesser Japanese moles.

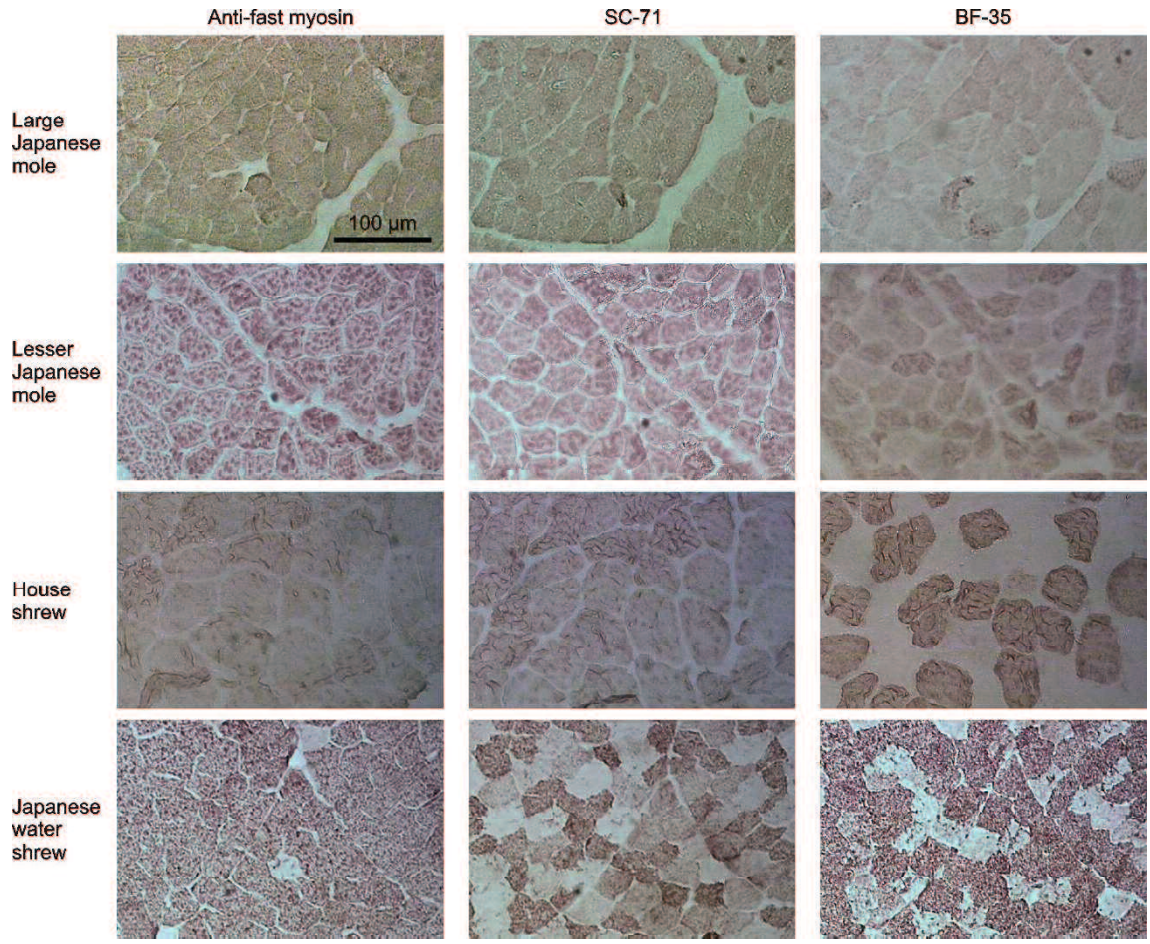

Fig. 2. Immunohistochemically-stained cross-sections of the vastus lateralis of four Soricomorpha species exhibiting different staining patterns. Scale bar is the same for all images.

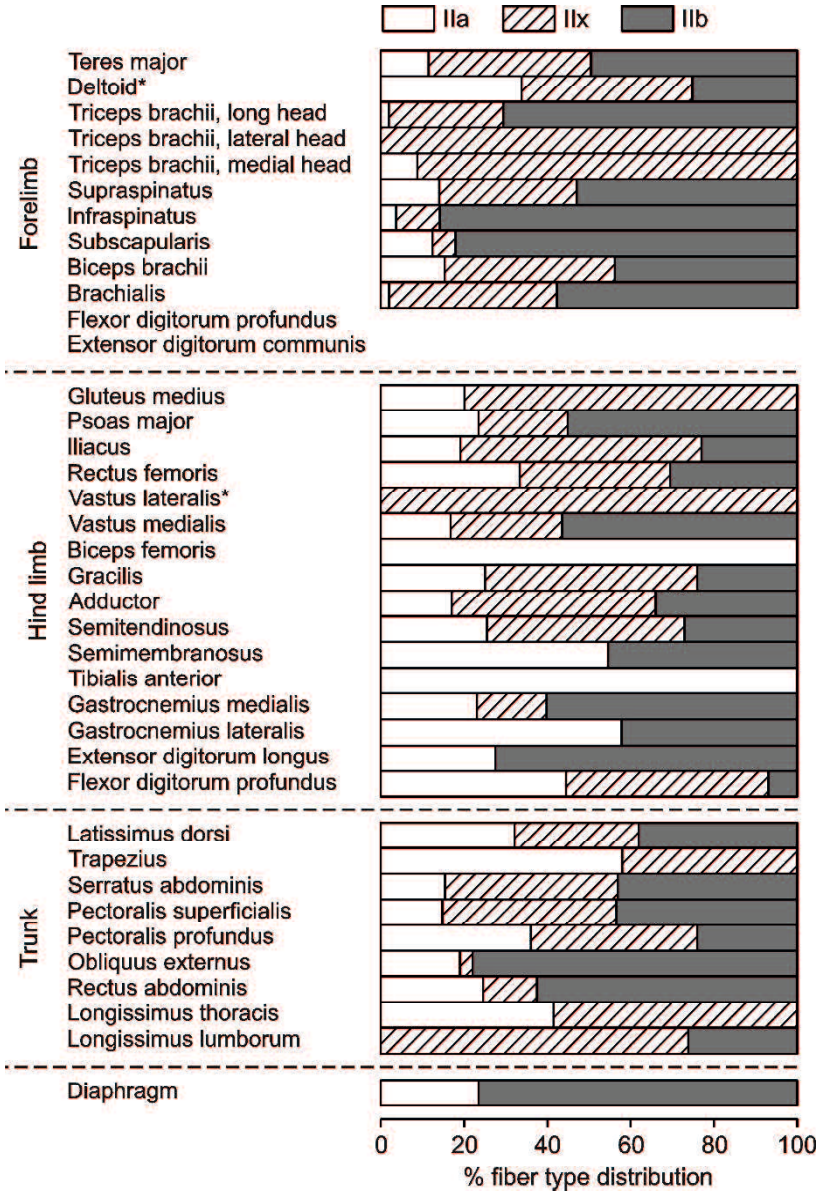

Fig. 3. Fiber type distribution percentage measured immunohistochemically in 36 muscles of the Japanese shrew-mole (*Urotrichus talpoides*). For the muscles marked with an asterisk, MHC distribution was further characterized electrophoretically.

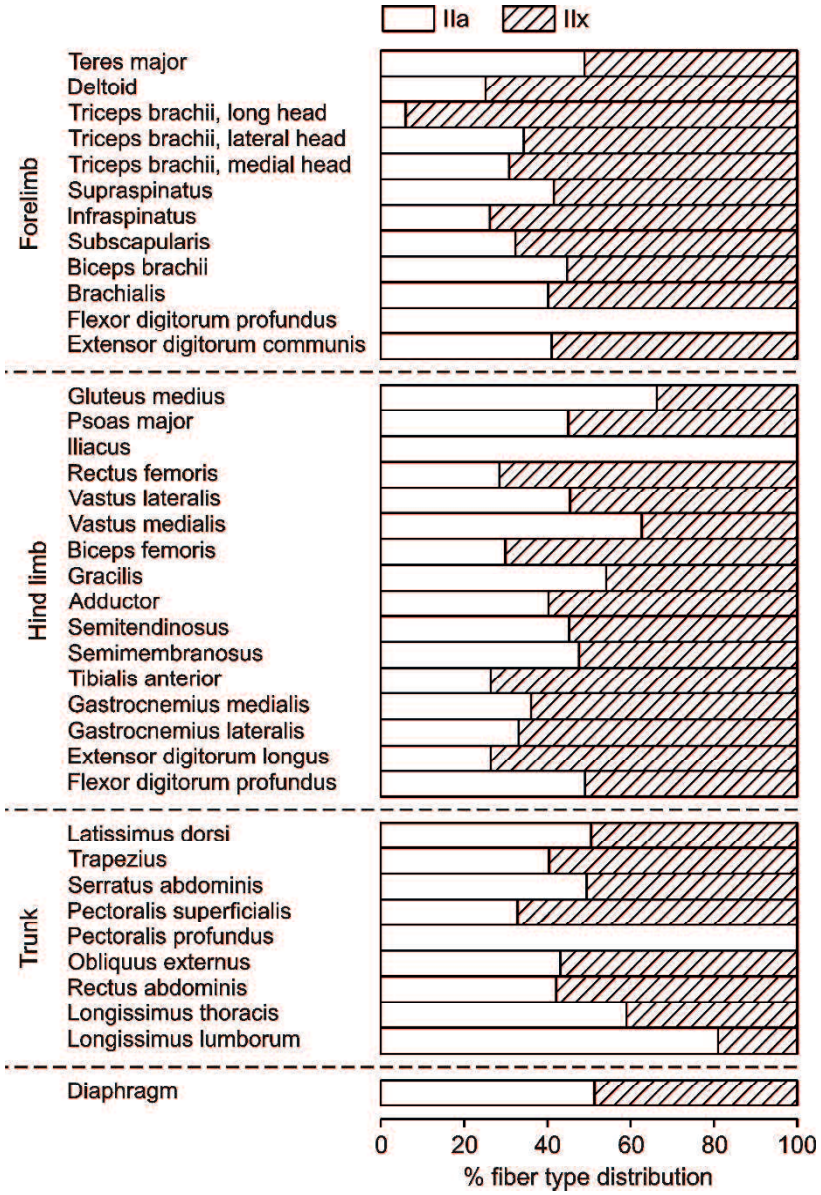

Fig. 4. Fiber type distribution percentage measured immunohistochemically in 38 muscles of the house shrew (*Suncus murinus*).

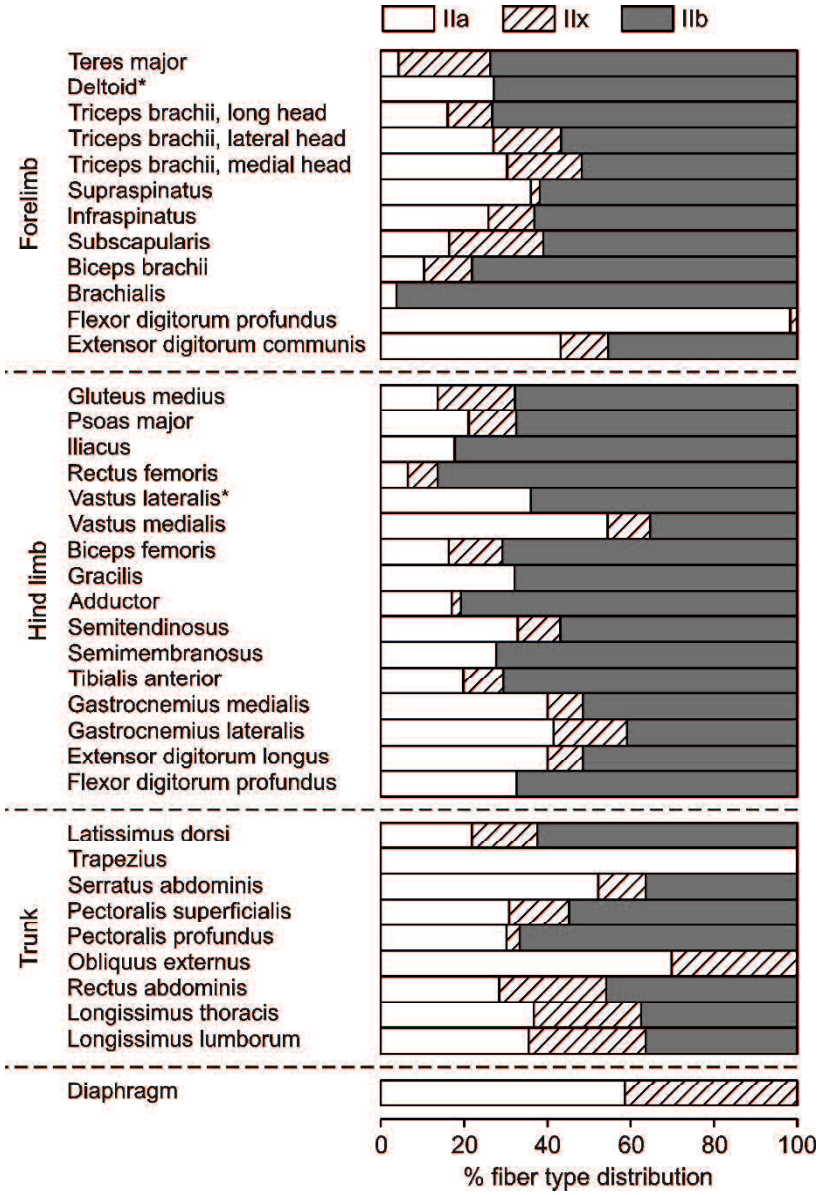

Fig. 5. Fiber type distribution percentage measured immunohistochemically in 38 muscles of the Japanese white-toothed shrew (*Crocidura dsinezumi*). For the muscles marked with an asterisk, MHC distribution was further characterized electrophoretically.

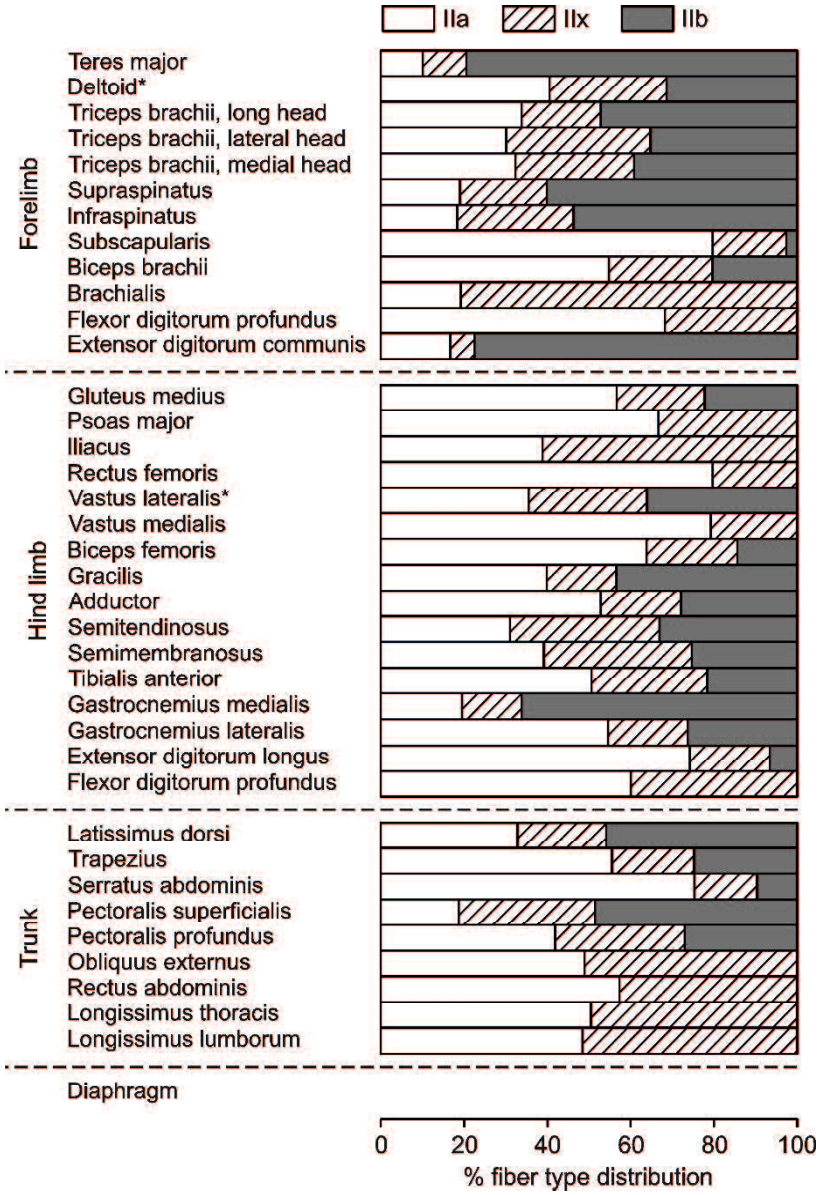

Fig. 6. Fiber type distribution percentage measured immunohistochemically in 37 muscles of the Japanese water shrew (*Chimarrogale platycephala*). For the muscles marked with an asterisk, MHC distribution was further characterized electrophoretically.

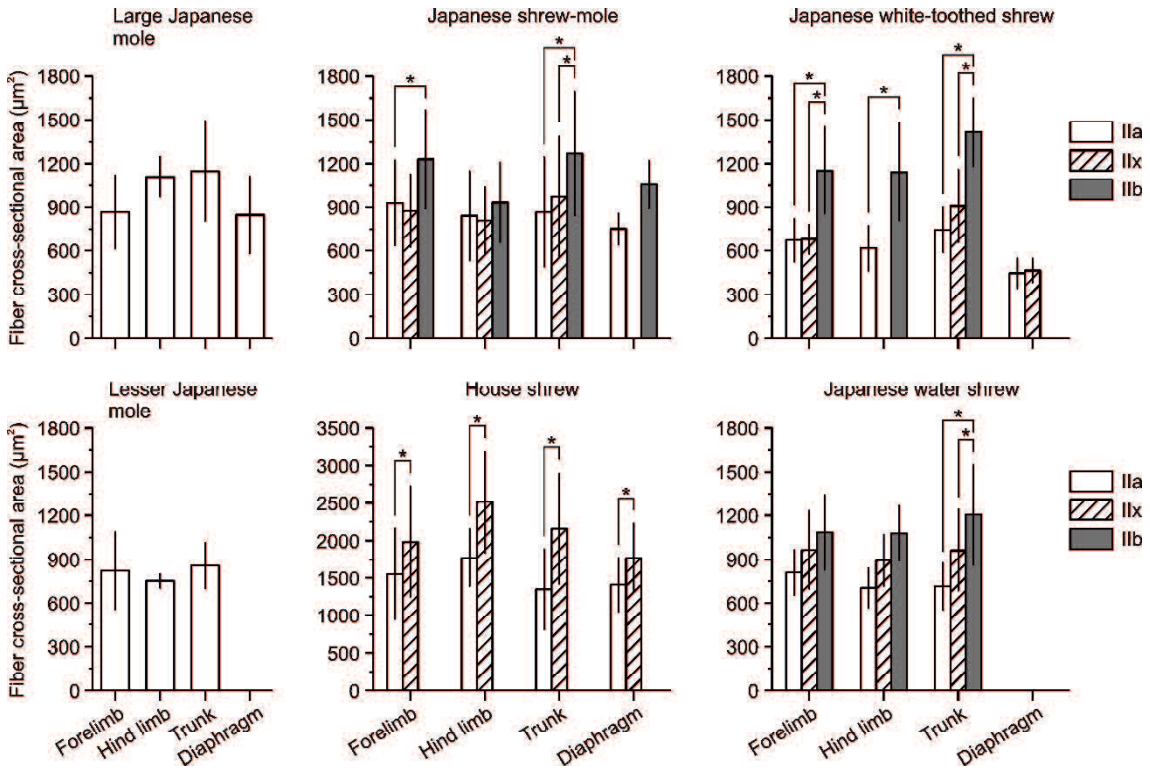

Fig. 7. Mean and standard deviation of fiber type cross-sectional area for six Soricomorpha species. Values are not presented for Type IIx fibers of muscles in the large Japanese mole and hind limb muscles in the Japanese white-toothed shrew because of the small percentage (<10%) of these fibers in each anatomical region. Note the different scale for the house shrew.

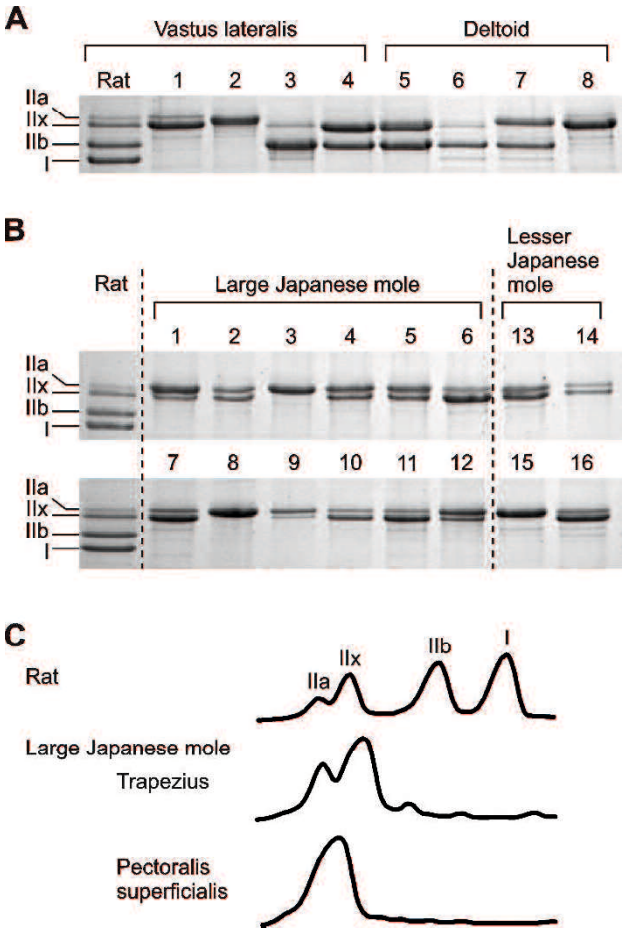

Fig. 8. Characterization of muscle fiber type distribution using gel electrophoresis. (A) SDS-PAGE results for the vastus lateralis and deltoid from four Soricomorpha species. On the left is a gel for the rat vastus lateralis that was used as an MHC isoform reference. Lanes 1 and 8: large Japanese mole, lanes 2 and 7: Japanese shrew-mole, lanes 3 and 6: Japanese white-toothed shrew, lanes 4 and 5: Japanese water shrew. (B) SDS-PAGE results for 12 muscles from the large Japanese mole and 4 muscles from the lesser Japanese mole. Lane 1: medial head of triceps brachii, lane 2: serratus abdominis, lane 3: infraspinatus, lane 4: long head of triceps brachii, lane 5: biceps brachii, lane 6: extensor digitorum communis, lane 7: trapezius, lane 8: pectoralis superficialis, lane 9: diaphragm, lane 10: biceps femoris, lane 11: gastrocnemius lateralis, lane 12: flexor digitorum profundus, lane 13: latissimus dorsi, lane 14: trapezius, lane 15: pectoralis superficialis, lane 16: gluteus medius. (C) Representative densitograms of the SDS-PAGE results for the trapezius and pectoralis superficialis from the large Japanese moles.

TABLE 1. Members of the order Soricomorpha used in this study

Taxa				Common name	Locomotor habits	No. of individuals	Body mass (g)	No. of muscles
Family Talpidae	Subfamily Talpinae	Tribe Talpini	*Mogera wogura*	Large Japanese mole	Strictly fossorial	2	98, 124	38
			Mogera imaizumii	Lesser Japanese mole	Strictly fossorial	1	65	13
		Tribe Urotrichini	*Urotrichus talpoides*	Japanese shrew-mole	Semi-fossorial	2	15.4, 17.0	36
Family Soricidae	Subfamily Crocidurinae		*Suncus murinus*	House shrew	Terrestrial	2	89, 112	38
			Crocidura dsinezumi	Japanese white-toothed shrew	Terrestrial	1	9.4	38
	Subfamily Soricinae		*Chimarrogale platycephala*	Japanese water shrew	Semi-aquatic	1	38.5	37

Classification after Wilson and Reeder (2005).

Common names after Ohdachi et al. (2015).

TABLE 2. Comparison of fiber type distribution among different anatomical regions in the large Japanese mole (*Mogera wogura*)

Characterization method	Region	No. of muscles	Muscle fiber type (%)			
			I	IIa	IIx	IIb
Immunohistochemistry	Forelimb	12	0.0 ± 0.0	98.9 ± 3.7	1.1 ± 3.7	0.0 ± 0.0
	Hind limb	16	0.0 ± 0.0	98.3 ± 6.9	1.7 ± 6.9	0.0 ± 0.0
	Trunk	9	0.0 ± 0.0	91.7 ± 24.9	8.3 ± 24.9	0.0 ± 0.0
Electrophoresis	Forelimb	6	1.1 ± 2.7	67.6 ± 26.8	30.7 ± 27.8	0.6 ± 0.9
	Hind limb	3	3.5 ± 7.0	51.5 ± 28.7	43.7 ± 35.0	1.3 ± 1.7
	Trunk	4	0.6 ± 1.1	58.7 ± 37.4	40.2 ± 36.0	0.5 ± 0.9

The data on the lesser Japanese mole were not presented because of the limited number of muscles studied.

The studies of muscle fiber distribution in moles show that most of all muscles in moles were mainly consist of type IIa muscle fibers. The muscle fiber composition of moles is very simple.

Summary-2

Contraction of skeletal muscle fibers is directly controlled by motor neurons. The axon of the motor neuron extends from the central nerve system including the brainstem and the spinal cord, and then branches and binds to the muscle fiber (neuromuscular junction). This system is called the motor unit and it is a combination of a motor neuron and a dominated muscle fiber.

The number of muscle fibers dominated by one motor neuron called "innervation ratio". If the innervation ratio is large, one motor neuron activates a large tension, and if the innervation ratio is small, the tension becomes small. The innervation ratio is an index indicating whether the change in tension is fine or rough. In general, the innervation ratio of the muscles of the fingertip is small, and that of the muscles of the thigh or the upper arm is large.

Motor units are classified as S（slow-twitch）,FR（fast-twitch fatigue resistant）,FI（fast-twitch intermediate）and FF（fast-twitch fatiguable）depending on the tension characteristics of the muscular fibers under the dominant nerve. Muscle fibers constituting S, FR, FI and FF may be regarded as Type I, IIa, IIx and IIb respectively.

Deference of motor units may reflect not only to the muscular fibers innervations but also in the properties of motor neurons. In other words, reactivity to input is different depending on the motor unit.

Elwood Henneman and his colleagues proposed the Size Principle of motor neuron recruitment which stated that for any net excitatory input to the motor neuron pool always from small to large. Stein and coworkers demonstrated that the size principle generalized to voluntary isometric contractions in humans, which they called Orderly Recruitment.

Motor neurons in motor unit classified S are easily excitable with inputs, and motor neurons in FF require more inputs good for excitement. Therefore, when the input reaches the motor neuron, it gets excited in the order of S, FR and FF. This is the concept of the recruitment order. Hoyte & Taylor also reported that the same phenomenon occurred also in locomotion.

That means, S unit is activated for low speed walks and FR and FF are activated respectively as the speed gets higher and the gait changes.

These findings indicate that tension control is performed by different type of movement units. However, we were very curious if the recruitment hypothesis could be applied to the tension control on moles of which composition of the muscle fibers is extremely simple and it would be predicted to be close to the on-off switching. Therefore, we examined characteristics of the tension of moles.

The Characteristics of Muscles in Moles - Relationship between muscle fiber distribution and twitch contraction-

Introduction

The purpose of the present experiments was to examine the physiological characteristics of muscles in moles, which are perfectly adapted to underground life.

In the preceding paper, we reported the simple muscle fiber distribution in muscles of moles (Ichikawa, in preparation). Most muscles in moles consisted only of type IIa muscle fibers, which are characterized by a larger potential force output and high fatigue resistance.

The muscle fibers in mammalian skeletal muscle are classified as type I, type IIa, type IIb, or type IIx, according to the specific isoforms of myosin heavy chains in sarcomeres and metabolic enzyme activity (Pette and Staron, 1993, 1997). Many mammalian muscles are composed of multiple types of muscle fibers (Agbulut et al., 2009; Arino et al., 1973; Cotton et al., 2008; Curry et al., 2012; Essen et al., 1975; Polgar et al., 1973; Schmidt and Schilling, 2007; Goto et al., 2013; Reichmann and Pette, 1982; Smerdu et al., 2009; Tonilo et al., 2007; Dearolf et al., 2000; Kielhorn et al., 2013; Suzuki et al., 1983; Williams and Noren, 2011; Hintz et al., 1980; Sugiura and

Murakami, 1990; Kohn et al., 2011; Kawai et al., 2009; Tonilo et al., 2007; Van Den Hoven et al., 1985, Haiya et al., 2013, Hazimihalis et al., 2013; Ohtsu & Uchida, 1979).

Contraction of the muscle fibers in skeletal muscles is caused by excitation of motoneurons. Motor units composed of a single motoneuron and muscle fibers is the elementary functional unit of motor response. Motor units are classified by muscle fiber type as S (Type I), FR (Type IIa), FI (Type IIx), or FF (Type IIb) units (Burke, 1991). Furthermore, the physiological properties (input resistance, duration following hyper-polarization, membrane time constant, and axonal velocity) of motoneurons and synaptic inputs for motoneurons are different depending on the type of motor unit (Burke, 1981). Therefore, excitability of motoneurons depends on motor unit type. Henneman (1981) reported that increased muscle force was achieved by increasing the number of activated motor units and the recruitment order of motor unit from S to FR and FI or FF in a steady contraction. Gillespie et al. (1974) found that in sudden movements, the fast-twitch units (FI or FF) were selectively activated. Savelberg (2000) suggested that the contraction phase and relaxation phase of twitch responses of single muscles were influenced by the fastest and slowest motor units in the muscle, respectively. Based on these reports, it is possible that fine control of muscle tension is difficult for muscles composed of one type of motor unit. In the previous paper, we

suggested that simple muscle fiber distribution in mole muscles is an adaptation to life that does not require sharp movements in tunnels. The purpose of this experiment was to confirm whether our hypothesis about tension control of muscles in moles stated above is correct. In order to clarify the characteristics of twitch response in mole muscles, we performed comparative studies with rats and H-shrews having similar weights as moles.

Materials and methods

Ethics Statement

All experimental procedures were reviewed and approved by the Animal Welfare and Ethics Committee of Yamaguchi University.

Animals

Experiments were performed using 20 adult Japanese moles (mole: Mogera wogura) (67-105 g), 18 adult rats (rat: Rattus norvegicus, Wistar line; BW: 240~320 g) and 15 adult Asian house shrews (H-shrew: *Suncus murinus*) (BW: 54~112 g). All samples included specimens of both sexes. The moles were harvested from the wild

with the permission of the Environment Preservation Division of Yamaguchi prefecture in Japan. The house shrews were bred at Okayama University of Science (Japan) and the rats were sourced from an experimental animal supplier (Kyudo, Japan).

Recording the tension of twitch contraction (Fig. 1)

Experimental animals were placed under general anesthesia with 50~60 mg/kg pentobarbital-Na solution i.p. (Nacalai Tesque, Japan). Tracheotomy was performed on each animal and tubes were inserted to allow voluntary ventilation. The experiments were performed within 2~3 hours. Rectal temperature was maintained at approximately 36°C using a heating lamp system (Nihon-Koden, Japan) and ECG was recorded. During experiments, one or two further injections of pentobarbital-Na (25~30 mg/kg, i.p.) were used to keep the animals in a stable condition. The left sciatic nerves were exposed after removal of the posterior biceps muscles. The sciatic nerve was separated carefully from surrounding tissue to allow electrical stimulation of the muscles of m triceps surae. The tendons originating from the three muscles in m. triceps surae (m. lateral gastrocnemius: LG, m. soleus: Sol, m. medial gastrocnemius: MG) were exposed and separated up to the muscle belly. The proximal part of the tibia was clamped using

forceps fixed to a stereotaxic frame. The tendons were cut distally and connected to a tension strain gauge with tungsten wire and the sciatic nerve was mounted on a bipolar stimulating electrode (Ag-AgCl, diameter: 0.3 mm, inter electrode distance 2.0 mm with cathode distally and anode proximally) at around mid-thigh level (Fig. 1A). A pool was formed by skin flaps and the nerve, allowing the electrode and muscles to be submerged in warmed mineral oil.

The sciatic nerve was stimulated with rectangular constant voltage pulses of 0.3 ms in duration. Threshold stimulation intensity (T) was defined as the voltage required to evoke the smallest observable twitch at 1/3 Hz. Stimulus intensities of 1.0T, 1.2T, 1.5T, 1.8T, 2T, 5T, and 10T were applied, and twitch responses were amplified via a transducer. Muscle tension and stimulus signal were acquired using a Power Lab recording device (AD instrumental, Australia). We measured the maximum active force ($F_{max)}$ in the averaged twitch contraction curve at different stimulus intensities. We also measured several values in an averaged twitch contraction curve at 2.0T (N=8): contraction time (Tco), relaxation time (Tre), half relaxation time (Tre-50%), late relaxation time (Tre-1/e), peak rate of force development (Fmax/Tco), and peak rate of relaxation (Fmax/Tre; Fig. 1B).

Histochemical Analysis

After recording the twitch responses in three kinds of muscles, animals were sacrificed with an overdose of pentobarbital-Na (95 mg/kg~) and dissected immediately. Samples of m. soleus (Sol), medial gastrocnemius (MG), and lateral gastrocnemius (LG) were excised whole from each individual, frozen in liquid nitrogen, and stored at -80°C until analysis. Four to eight 10-μm thick cross-sections were obtained from each block of frozen muscle using a cryostat (Leica, Nusslock, Germany) at −20°C. The sections were thawed to room temperature and then preincubated in goat normal serum in 0.2 M phosphate buffer (pH 7.6) at 25°C for 10 min before application of primary monoclonal antibodies raised against: (1) MHC fast myosin, which reacts specifically with MHC-II; (2) SC-71, to label MHC-IIa and (3) BF-35m to label no-MHC-IIx. The sections were incubated at 25°C for 180 min, washed with phosphate buffer, and then incubated for a further 180 min at 25°C with a secondary antibody conjugated with horseradish peroxidase. Tissues were then washed again with phosphate buffer. The secondary antibodies were reacted using Diaminobenzidine tetrahydrochloride as a chromogen to visualize the conjugated peroxidase (Kawai et al., 2009). Images of the stained muscle fibers were obtained by microscopy (Nikon E600, Tokyo, Japan) with an image-processing system (Nikon DS-U1, Tokyo, Japan). The immunohistochemically

stained micrographs allowed muscle fibers to be classified as type I, type IIa, type IIx or type IIb, and the percentage of each type was calculated from counts of 500 fibers from three animals. Type I fibers characteristically stain weakly with both anti-MHC fast and SC-71. Type IIa has a high affinity for both anti-MHC fast and SC-71. Type IIx fibers are stained strongly by anti-MHC fast, and weakly by SC-71 and BF-35. Type IIb stain strongly with anti-MHC fast and BF-35, and weakly with SC-71. Cross-sectional areas (CSA) were measured for at least 25 muscle fibers of each type.

Calculation of PCSA

We measured the weight of whole muscle (MW: mg), fiber length (FL:mm), and angle of pinnate fibers (α) in LG, MG, and Sol in five rats, three H-shrews, and three moles to calculate the physiological cross-sectional area (PCSA =MW·cos α/ 1.06·FL, Friederich and Brand, 1990; Mendez and Keys, 1960).

Statistical Analysis

Mean values for measured values are given as ± the standard of the mean (SEM). Significance ($P<0.05$) was determined using ANOVA followed by a Tukey test ($p<0.05$).

Results

Twitch response

Figure 2 shows representative averaged twitch responses from MG muscle of rat, H-shrew and mole at 1.0T~2.0T. Increasing the stimulus intensity led to an increase in Fmax.

Table 1 shows the Fmax at 1.0~2.0T as a percentage of Fmax at 2T. In all muscles for all species studied, Fmax increased by increasing the stimulus intensity. The Fmax in all muscles markedly increased between 1.0T and 1.2T, and 1.2T and 1.5T. Fmax in LG in all studied animals markedly increased between 1.0T and 1.2T. Fmax reached a maximum at 1.8T or 2.0T in all studied animal muscles, and further increasing of stimulus intensity did not change the Fmax.

Table 2 shows the Fmax (mN), Fmax/MW (mN/mg), Tco (ms), Tre-50% (ms), Tre-1/e (ms), Fmax/Tco (N/s), and Fmax/Tre (N/s) of averaged twitch response at 2.0T. Fmax of MG, LG, and Sol at 2.0T in rats was much greater than in either H-shrew or mole, whereas force per muscle weight (Fmax/MW) of MG and LG in moles was greater than in rats. Fmax/MW in Sol was the highest in H-shrews. Mole muscles (LG and MG) produce the greatest tension per muscle weight.

The Tco of all three muscles was greatest in the mole, and lowest in the H-shrew. Tre of MG and LG were longest in the mole, but there was no significant difference in Sol among species. Tre-50% was greatest in the mole, and Tre-1/e were lowest in the H-shrew.

The peak rate of development and relaxation rate of twitch response of all three muscles (Fmax/Tco, Fmax/Tre) were lowest in moles and largest in rats.

Muscle fiber distribution

Table 3 shows the percentage population (%) of fiber types I, IIa, IIx, and IIb in MG, LG, and Sol of rat, H-shrew and mole. In rat, the MG and LG consisted mainly of type IIb (MG: 64.2%, LG: 64.8%) and type IIx (MG: 33.8%, LG: 28.2%) fibers, while Sol comprised mainly type I (81.0%). The muscles of H-shrews consisted of type IIa and IIX muscle fibers (MG: IIa: 36.1%, IIx: 63.9%; LG: IIa: 33.1%, IIx: 66.9%; Sol: IIa: 66.9%, IIx: 33.1). In moles, all muscles were formed exclusively of type IIa fibers.

Table 4 shows the averaged cross-sectional area (CSA: mean ± SD μm^2) of each fiber type the in studied muscles, ranging from 2130 to 4357 μm^2 in rats, 1550 to 2271 μm^2 in H-shrews, and 1247 to 1343 μm^2 in moles. CSAs of type IIb fibers in MG and

LG were larger than those of type IIa. In H-shrews, CSAs of type IIa in LG were larger than those of type IIx, but no significant difference in CSA was observed in MG or Sol.

PCSA

Table 7 shows the averaged values of muscle weight (MW:mg), fiber length (FL:mm), angle of pinnate fibers (α0), and PCSA of MG, LG, and Sol in three animals. MW, FL, and PCSA of muscles in moles were markedly smaller than in H-shrews and rats.

Discussion

Some investigators reported that a mixed population of muscle fiber types permits fine control of muscle force (Hennneman, 1981; Burke, 1981, 1990, Zajac and Faden, 1985; Savelberg, 2000; Gillespie et al., 1974). The majority of mammalian muscles are composed of more than one type of muscle fiber, and innervated by different types of motoneurons (Essen et al., 1975; Johnson et al., 1973; Reichmann & Pette, 1982; Schmidt & Schilling, 2007; Goto et al., 2013; Reichmann and Pette, 1982; Ariano et al., 1973; Tonilo et al., 2007; Cotton et al. 2008; Dearolf et al., 2000; Kielhorn

et al., 2013; Suzuki et al., 1983; Williams and Noren, 2011; Agbulunt et al., 2009; Hintz et al., 1980; Curry et al., 2011; Kawai et al., 2009; van den Hoven et al., 1985; Haiya et al., 2013). Our histological studies of muscle fiber distribution in moles revealed that muscles in mole consist of only type IIa. This suggests that the tension control of muscles in moles is very simple. In the previous paper, we concluded that the simple muscle fiber distribution in mole muscles is an adaptation to the environment in tunnels (Ichikawa et al. in preparation). The purpose of the present experiments was to verify our hypothesis that tension control of mole muscles is very simple.

In the present experiments, we employed electrical stimulation to stimulate muscle nerves. Some investigators reported differences in the axonal conduction velocity and axonal diameter depending on the motor unit types (Burke, 1981). Under electrical stimulation, faster motor units are activated first, and slower motor units were recruited as the intensity of the stimulus increased. Therefore, the increase in Fmax by increasing the stimulus intensity is likely due to recruitment of different types of motor units. For the mole, all muscles and motor units comprise only type IIa muscle fibers (Table 3). Thus, the twitch response of muscles is expected not be increased by increasing the intensity of electrical stimulation. However, the present experiments demonstrated that the Fmax was increased by increasing stimulus intensity in all studied

species regardless of muscle fiber distribution. This suggests the existence of functional differentiation in FR units (type IIa) in mole muscles, and moles likely have a neuronal control system to selectively use parts of FR units.

Fmax at 2.0T was largest in rats. However, the Fmax per muscle weight (Fmax/MW) was lowest in rats and largest in moles (Table 2). Weights of m. triceps surae in rats, H-shrews, and moles are approximately 0.90%, 0.17%, and 0.12% of the body weight, respectively. Thus, moles produce a larger tension with a small mass of muscle. The muscle fiber length (FL) and pinnate angle (α), in addition to muscle weight, are involved in muscle tension. PCSA calculated from MW, FL, and α has been used to estimate the maximum tension of muscle (Friederich and Brand, 1990; Mendez and Keys, 1960). The short FL and small α can be considered as causes of the large tension per muscle weight in mole muscles. The maximum muscle stress used to calculate the maximum tension from PCSA was reported to differ among muscles and species (Usami, 2014). Great maximum muscle stress (N/cm2) may be a cause of the larger Fmax/MW in moles.

Tco and Tre in the maximum twitch response depend on the fastest and slowest muscle fibers, respectively (Savelberg, 2000). The fastest muscle fibers are type IIb in rats (MG: 64.2%; LG: 64.8%; Sol: 6.9%), type IIx in H-shrews (MG: 63.9%; LG:

66.9%; Sol: 33.1%) and type IIa in moles (MG: LG: Sol: 100.0%). For all muscle types studied, T_{co} values were greater in moles than in rats and H-shrews. However, Tco values were the lowest in H-shrews. The slowest muscle fibers were type IIa in moles (MG: LG: Sol: 100.0%) and H-shrews (MG: 36.1%; LG: 33.1%; Sol: 66.9%), and MG in rats (MG: 2.0%), and type I in LG (2.0%), Sol (81.0%) in rats. Tre values in all muscles were largest in moles. Tre-50% values tended to be the same as Tre, but these results are partially inconsistent with the theory by Savelberg. As the Fmax depends on the muscle and species, we evaluated the relationship between muscle fiber distribution and contraction rate (Famx/Tco) and relaxation rate (Fmax/Tre) to clarify the relationship between muscle fiber distribution for contraction and relaxation of twitch response. According to the theory by Savelberg (2000), Fmax/Tco should reflect the contraction time of the fastest muscle fibers in the muscles, whereas Fmax/Tre should reflect the relaxation time of the slowest muscle fibers. Fmax/Tco was lower in the order of mole, H-shrew and rat. This suggests that the fastest fiber type in muscle affects Fmax/Tco. However, there is no association between the degree of muscle fiber distribution and Fmax/Tco. For example, the distribution of type IIb fibers in both the MG and LG of rats was 65%, but the Fmax/Tco in the MG and LG were significantly different. The slowest muscle fibers were type IIa in moles and H-shrews, and in MG in

rats, and type I in LG and Sol in rats. Values of Fmax/Tre in the three studied muscles are similar in moles and H-shrews. Fmax/Tre in the MG tended to be lower than that in the LG and Sol. Our results partly support the theory by Savelberg (2000). The muscle fiber distribution and values shown in Table 3 suggest that the physiological characteristics of the same motor units are different depending on muscles and animals.

The experiments described here attempted to clarify the relationship between twitch contraction of muscle and the muscle fiber distribution. Many studies have found that the existence of different types of muscle fibers permits fine control of muscular force and contraction speed (Burke, 1981, 1990; Henneman, 1981; Savelberg, 2000). The present experiment is partly in agreement with the previous theory. As Savelberg reported, the temporal characteristics of the twitch response are related with muscle fiber distribution. We demonstrated the existence of recruitment order within the same motor units. Thus, the same motor units in moles may be finely differentiated. Further studies on the physiological characteristics of motoneurons are necessary to understand the recruitment order in FR motor units in moles.

References

Agbulut O, Vignaud A, Hourde C, Mouisel E, Fougerousse F, Butler-Brouwn SG, Ferry A (2009) Slow myosine heavy chain expression in the absence of muscle activity. Am J Physiol Cell Physiol 296: C205-C214

Ariano MA, Armstrong RB, Edgerton VR (1973) Hindlimb muscle fiber populations of five mammals. J Histochem Cytochem 21: 51-55

Burke RE (1981) Motor units: Anatomy, physiology, and functional organization, In: Brookhar, J.M., Mountcastle, V.B (eds) Handbook of Physiology, Sec 1, Vol. II, Pt. 1, The Nervous System: Motor Control, American Physiological Society, pp345-422

Burke RE (1990) Spinal cord: ventral horn. In Shephaerd G.E.(ed) The Synaptic Organization of The Brain. Oxford University Press, pp 88-132

Cotton BP, Piscitelli AM, McLellan AW., Rommel AS, Dearolf LJ, Pabst AnnD (2008) The gross morphology and histochemistry ofrespiratory musclesin bottlenose dorphins,Tursiopstruncatus. J Morphol 269*1520-1538

Curry WJ, Hohl R, Noakes DT, Kohn AT (2012) High oxidative capacity and type IIx fiber content in springbok and fallow deer skeletal muscle suggest fast sprinters with a resistance to fatigue. J Exp Biol 215:3997-4005

Dearolf LJ, McLellan AW, Dillaman MR, FriersonJr A, Pabst AnnD (2000) Precocial development of axial locomotor musclein bottlenose dolphins (Tursiops truncates).J Morphol 244:203-215

Essen B, Jansson E, Henriksson J (1975) Metabolic characteristics of fibre types in human skeletal muscle. Acta Physiol Scand 95:153-165

Fang ZP, Mortimer JT (1991a) Selective activation of small motor axons by quasi-trapezoidal current pulses. IEEE Transactions on Biomedical Engineering 38: 168-175

Fang ZP, Mortimer JT (1991b) A method to effect physiological recruitment order in electrically activated muscle. IEEE Transactions on Biomedical Engineering, 38: 175-179

Friederich AJ, Brand AR (1990) Muscle fiber architechture in the human lower limb. J Biamechanics 23:9-95.

Goto M, Kawai M, Nakata M, Itamoto K, Miyata H, Ikebe Y, Tajima, T, Wada N (2013) Distribution of Muscle Fibers in Skeletal Muscles of the Cheetah (Acinonyx jubatus). Mam Biol 78:127-133

Haiya M, Une S, Kawada M, Itamoto K, Tani Y, Miyata H, Kihara I, Mori F, T.ajima T, Wada N (2013) Distribution of Muscle Fibers in Skeletal Muscles of the African Elephant (Loxodonta africana africana). Mamm Study 38: 135-140.

Henneman E (1981) Recruitment of motoneurons: The size principle. In Desmedt JE(ed) Motor Unit Types, Recruitment and Plasticity in Health and Disease, Vol 9 Progress in Clinical Neurophysiology, Basel, Karger, pp26-60

Hintz CS, Lowry CV, Kaiser KK, Mckee D, Lowry OH (1980) Enzyme levels in individual rat muscle fibers. Am J Physiol Cell Ph 239:C58-C65

Johnson MA, Polgar J, Weightman D, Appleton D (1973) Data on the distribution of fiber types in thirty-six human muscles-An autopsy study. J Neursci 18:111-129

Kawai M, Minami Y, Sayama Y, Kuwano A, Hiraga A, Miyata H (2009) Muscle fiber population and Biochemical properties of whole body muscles in thoroughbred horses. Anat Rec 292:1663-1669

Kielhorn EC, Dillaman RM, Knsey TS, McLellan AW, Gay MD, Dearolf J, Pabs AD (2013) Locomotor muscle profile of a deep (Kogia breciceps) versus shallow (Tursiops Truncatus) diving cetacean. J Morphol 274:663-675.

Mendez J, Keys A (1960) Density and composition of mammalian muscle. Metabolism 9: 184–188

Pette D, Staron RS (1993). The molecular diversity of mammalian muscle fibers. News Physiol Sci 8:153-157.

Pette D, Staron RS (1997) Mammalian skeletal muscle fiber type transitions. Int Rev Cytol 170:153-157

Reichmann H, Pette D (1982) A comparative microphotometric study of succinate dehydrogenase activity levels in type I, IIA and IIB fibers of mammalian and human muscles. Histochem 74:27-41

Savelberg (2000) Rise and Relaxation times of twitches and tetani in submaximally recruited, mixed muscle: A computer model. In Herzog W (ed), Skeletal Muscle Mechanics、John Wiley & Sons, pp225-240

Schiaffino S, Reggiani C (1994) Myosin isoforms in mammalian skeletal muscle. J Appl Physiol 77:493-501

Schmidt, M., Schilling, N., 2007. Fiber type distribution in the shoulder muscles of the tree shrew, the cottom-top tamarin, and the squirrel monkey related to shoulder movements and forelimb loading. J. Hum. Evol. 52, 401-419.

Suzuki A, Tsuchiya T, Takahashi Y, Tamate H (1983) Histochemical properties of myofibers in longissimus muscle of common dolphins (Delphinus Dephis). Acta Histochem Cytochem 16:223-231

Tonilo L, Maccatrozzo L, Patruno M, Pavan E, Caliaro F, Rossi R, Rinaldi C, Canepari M, Reggiani C, Mascarello F (2007) Fiber types in canine muscles: myosin isoform expression and functional characterization. Am J Physiol_Cell Ph 292:C1915-1926

van den Hoven R, Wensing T, Breukink H, Meijer A E, Kruip TA (1985) Variation of fiber types in the triceps brachii, longissimus dorsi, gluteus medius, and biceps femoris of horses. Am J Vet Res 46: 939-941

Williams MT, Noren RS (2011) Extreme physiological adaptation as predictors of climate-change sensitivity in the narwhal. Mar Mammal Sci 27:334-349

Zajac FE, Faden JS (1985) Relationship among recruitment order, axonal conduction velocity, and muscle-unit properties of type-identified motor units in cat plantaris muscle. J Neurophysiol 53:1303-1322

Figure legends

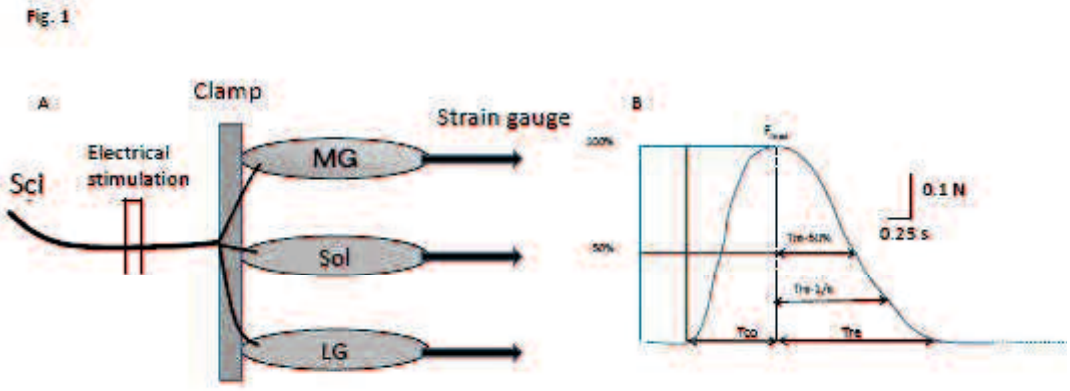

Fig. 1A: Experimental set-up. The common tibial nerve was stimulated. The Achilles tendons for MG, LG, and Sol were fixed to a strain gauge with tungsten wire.

Fig. 1B: Measuring the peak amplitude (Fmax), duration of rising phase (Tco) and duration of relaxation phase (Tre) of the twitch response. The times taken to achieve relaxation phases, half-relaxation time (Tre-50%), and late relaxation time (Tre-1/e) were also measured.

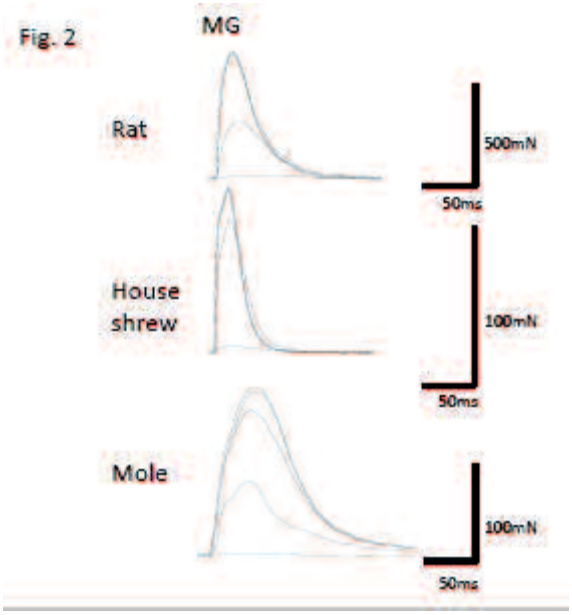

Fig. 2: Representative twitch response in MG, LG, and Sol of rats at 1.0T, 1.2T, 1.5T, 1.8T and 2.0T. Each curve is the average of eight twitch responses. Increasing the stimulus intensity increased the amplitude of the twitch response, and maximum amplitude was achieved above 1.8~2.0T.

Table 1: Fmax at 1.0~2.0T as a percentage of Fmax at 2T (mean ±SD). * <0.05

Table. 1

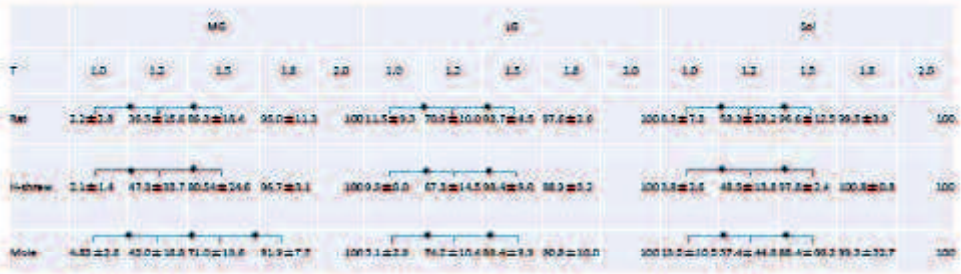

Table 2: Averaged values of twitch responses at 2.0T.

Fmax: maximum contraction force; Fmax/MW: the tension per muscle mass, Tco: contraction time; Tre: relaxation time; Tre-50%: half-relaxation time; Tre-1/e: Late-relaxation time (37%); Fmax/Tco: peak rate of force development; Fmax/Tre: peak rate of relaxation

Table. 2

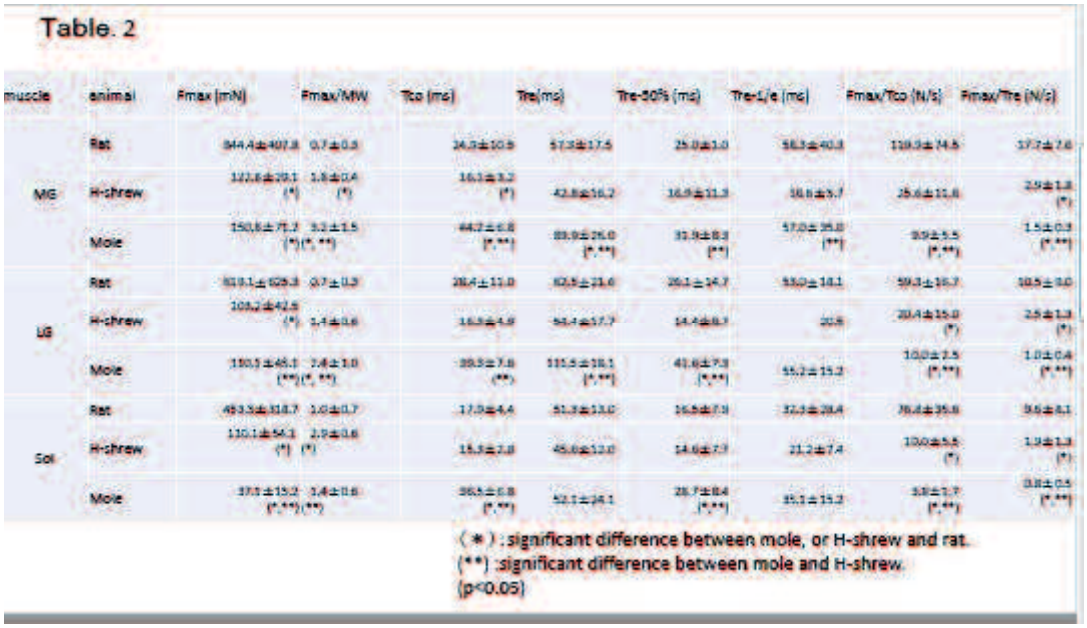

(＊) : significant difference between mole, or H-shrew and rat.
(**) :significant difference between mole and H-shrew.
($p<0.05$)

Table 3: The distribution (%) of type I, IIa, IIx, and IIb muscle fibers in MG, LG, and Sol of rat, house shrew, and mole.

Table 3

Muscle fiber distribution

	MG				LG				Sol			
%	I	IIa	IIx	IIb	I	IIa	IIx	IIb	I	IIa	IIx	IIb
Rat	0.0	2.0	33.8	64.2	2.0	5.0	28.2	64.8	80.6	12.7	0.0	6.7
H-shrew	0.0	36.1	63.9	0.0	0.0	33.1	66.9	0.0	0.0	66.9	33.1	0.0
Mole	0.0	100.0	0.0	0.0	0.0	100.0	0.0	0.0	0.0	100.0	0.0	0.0

Table 4: Averaged cross-sectional area (mean ± SD μm^2) of different muscle fiber types.

Table 4

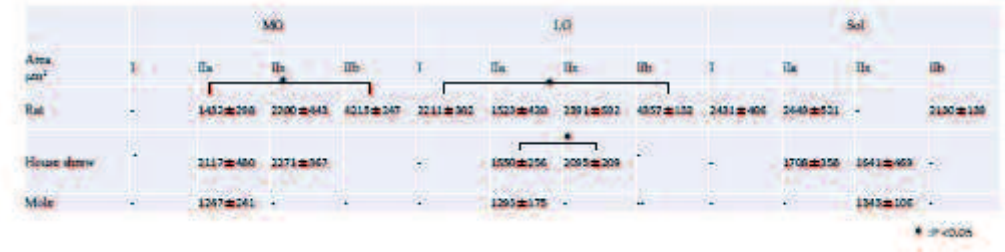

Table 5: The muscle weight, fiber length, cos α (α: pennate angle), PCSA, and PCSA/MW (cos α/1.06FL).

Table 5
Averaged muscle weight (MW mg), fiber length (FL,mm), pennate angle (α), PCSA (cm^2) and PCSA/BW(body weight)

animal	muscle	MW (mg)	FL (mm)	α (°)	PCSA (cm^2)	PCSA/BW (cm^2/Kg)
Rat	MG	1272.4 ± 256.1	9.37 ± 1.99	18.13 ± 2.81	1.15 ± 0.31	2.60 ± 0.35
	LG	917.9 ± 405.3	9.37 ± 1.25	18.93 ± 2.39	0.91 ± 0.50	1.96 ± 0.61
	Sol	437.5 ± 102.9	8.64 ± 0.79	15.47 ± 4.10	0.46 ± 0.13	1.04 ± 0.10
House shrew	MG	66.7 ± 11.2	5.26 ± 1.06	15.07 ± 11.67	0.12 ± 0.02	1.88 ± 0.37
	LG	75.5 ± 14.3	5.97 ± 1.99	16.59 ± 23.69	0.11 ± 0.03	1.81 ± 0.49
	Sol	37.3 ± 11.2	5.93 ± 2.05	17.07 ± 22.22	0.06 ± 0.02	0.90 ± 0.30
Mole	MG	46.7 ± 17.5	4.66 ± 0.96	12.28 ± 6.97	0.06 ± 0.03	0.70 ± 0.43
	LG	45.3 ± 22.7	6.19 ± 1.59	11.06 ± 2.76	0.04 ± 0.01	0.39 ± 0.13
	Sol	26.6 ± 10.9	5.13 ± 0.81	6.67 ± 4.25	0.03 ± 0.004	0.34 ± 0.001

* $P < 0.05$

Summary-3

The results of the present experiments show that the tension control of mole's muscles is significantly different from tension control of other muscles. The most of all mammals control tension of various muscles by adding motor units with different tension properties (S, FR, FI, FF: Henneman's Principle). However, mole control muscle tension by increasing the activated muscle fibers with uniform tension characteristics. Motoneurons that innervate uniform muscle fibers have different electrophysiological characteristics.

Acknowledgments

I am grateful to the following professors and researchers for their guidance to conduct this research.

Prof. N. Wada (Yamaguchi University)

Dr. S. Kawada (National Science Museum)

Dr. H. Tanaka (Museum of Yamaguchi Prefecture)

Prof. H. Miyata (Yamaguchi University)

Prof. Y. Yamano (Tottori University)

Prof. M. Nakaichi (Yamaguchi University)